To the Graduate Council:

I am submitting herewith a dissertation written by Mary Kaye Geck entitled "Characterization of the Thioredoxin-Modulated Regulation of Fructose-1,6-Bisphosphatase, NADP-Dependent Malate Dehydrogenase, and Phosphoribulokinase." I have examined the final copy of this dissertation for form and content and recommend that it be accepted in partial fulfillment of the requirements for the degree of Doctor of Philosophy, with a major in Biomedical Sciences.

Fred C. Hartman, Major Professor

We have read this dissertation
and recommend its acceptance:

Accepted for the Council:

Associate Vice Chancellor and
Dean of The Graduate School

CHARACTERIZATION OF THE THIOREDOXIN-MODULATED REGULATION OF FRUCTOSE-1,6-BISPHOSPHATASE, NADP-DEPENDENT MALATE DEHYDROGENASE, AND PHOSPHORIBULOKINASE

A Dissertation
Presented for the
Doctor of Philosophy
Degree
The University of Tennessee, Knoxville

Mary Kaye Geck
August 1997

DEDICATION

To my family

ACKNOWLEDGMENTS

I sincerely acknowledge the tremendous contributions of my major advisor, Dr. Fred C. Hartman, to my graduate research. He was always there whenever I needed guidance, his patience and moral support were unyielding, and he has provided a wonderful example of professionalism. It was truly a privilege to work with him.

I am grateful to Dr. Salil Niyogi for not only serving on my dissertation committee but for also sparking my interest in protein engineering. While spending a summer and a semester in his lab during my undergraduate years, I first became directly exposed to the field and learned several techniques that I was later able to transfer to this dissertation research. I am also grateful to Dr. Frank Larimer and the members of his laboratory, Shen Lu and Alice Hardigree, for the large part they played in the molecular biology aspects of this project. Their expertise provided a springboard for troubleshooting several aspects of molecular cloning and mutagenesis. Dr. Larimer's assistance with structural analysis, including the generation of the thioredoxin structures presented herein, is greatly appreciated. I would also like to thank the rest of my committee members: Drs. Jorge Churchich, Margaret Terzaghi-Howe, and Richard Mural. They each provided a unique perspective on this project and were very supportive.

The assistance of the other members of Dr. Hartman's laboratory also needs to be recognized. The contributions of Dr. Hillel Brandes were numerous and ranged from offering advice to sharing precious supplies. His expertise played an extensive role in making progress with this project possible. Claude Stringer operated the protein sequencer, allowing for the amino acid sequences described in Chapters 2 and 4 to be determined. The advice and support of Drs. Mark Harpel and Yuh-Ru Chen were also invaluable.

Financial support for this work has been provided by the U.S. Department of Agriculture under grants 94-37306-0337 and 96-35306-3412 from the National Research Initiative Competitive Grants Program, the U.S. Department of Energy under contract DE-AC0596OR22464 with Lockheed Martin Energy Research, and the University of Tennessee-Knoxville.

ABSTRACT

Two chloroplastic thioredoxins, denoted Trx *f* and Trx *m*, mediate photosynthetic light regulation of carbon dioxide assimilation via modulation of the redox status of certain target enzymes. The necessity for distinct chloroplastic thioredoxins has been viewed as reflective of their differential selectivities for these target enzymes. Trx *f* has been reported to be selective for fructose-1,6-bisphosphatase (FBPase), phosphoribulokinase (PRK), sedoheptulose-1,7-bisphosphatase, and NADP-linked glyceraldehyde 3-phosphate dehydrogenase. Trx *m*, on the other hand, has appeared to be selective for NADP-dependent malate dehydrogenase (MDH) and chloroplastic glucose 6-phosphate dehydrogenase.

One objective of this project was to identify recognition and selectivity determinants of Trx *f*. Amino acid sequence alignments and three-dimensional structures of *E. coli* Trx were used to identify residues of Trx *f* that appear to be unique and accessible for interaction with target enzymes. These Trx *f* residues were then replaced with those found at corresponding positions of Trx *m*, resulting in the following site-directed mutants: K58E, Q75D, N74D, the deletion mutants ΔAsn74 and ΔAsn77, T105I, and the double mutant V89I/T105I. Through kinetic analyses of the mutants constructed, Lys58, Asn74, Gln75, and Asn77 of Trx *f* were found to contribute to its interactions with FBPase and MDH and influence target enzyme selectivity. Val89 and Thr105 were also determined to be important for binding to FBPase. However, contrary to literature reports, wild-type Trx *f* is superior to wild-type Trx *m* in the activation of both FBPase and MDH. Furthermore, the wild-type and mutant thioredoxins display similar efficiencies in the activation of PRK. Thus, the physiological basis for the two thioredoxins cannot be explained on the basis of differential target enzyme specificity as heretofore accepted.

A second objective of this project was to ascertain the feasibility of using fluorescence anisotropy to directly measure the binding affinities of the thioredoxins for their target enzymes. For this purpose, the wild-type chloroplastic thioredoxins were fluorescently labeled with isatoic anhydride. The affinity (K_d) of derivatized Trx *f* for PRK was only twice as large as the apparent affinity value determined by kinetic analyses. In addition, the K_d values for derivatized Trx *f* and *m* for PRK differed by only two-fold. Derivatization, however, greatly impaired the ability of the thioredoxins to activate their targets. Thus, a residue involved in Trx-target enzyme interaction may have been modified.

TABLE OF CONTENTS

LIST OF FIGURES

LIST OF ABBREVIATIONS

Amino acids	Ala or A, alanine	Leu or L, leucine
	Arg or R, arginine	Lys or K, lysine
	Asn or N, asparagine	Met or M, methionine
	Asp or D, aspartate	Phe or F, phenylalanine
	Cys or C, cysteine	Pro or P, proline
	Gln or Q, glutamine	Ser or S, serine
	Glu or E, glutamate	Thr or T, threonine
	Gly or G, glycine	Trp or W, tryptophan
	His or H, histidine	Tyr or Y, tyrosine
	Ile or I, isoleucine	Val or V, valine

ATP	adenosine 5´-triphosphate
Bicine	N,N´-bis-(2-hydroxyethyl)glycine
BME	2-mercaptoethanol
BSA	bovine serum albumin
DTNB	5,5´-dithiobis-(2-nitrobenzoic acid)
DTT	dithiothreitol
E. coli	*Escherichia coli*
EDTA	ethylenediaminetetraacetic acid
ELISA	enzyme-linked immunosorbent assay
FAD	flavin adenine dinucleotide
FBP	fructose 1,6-bisphosphate
FBPase	fructose-1,6-bisphosphatase
FTR	ferredoxin-thioredoxin reductase
GAPDH	glyceraldehyde 3-phosphate dehydrogenase

GSH	reduced glutathione
GSSG	oxidized glutathione
HEPES	N-(2-hydroxyethyl)piperazine-N´-(2-ethanesulfonic acid)
HPLC	high-performance liquid chromatography
IPTG	isopropyl-β-D-thiogalactopyranoside
kDa	kilodalton
MDH	NADP-dependent malate dehydrogenase
NAD(H)	nicotinamide-adenine dinucleotide (reduced)
NADP(H)	nicotinamide-adenine dinucleotide phosphate (reduced)
NMR	nuclear magnetic resonance
NOE	nuclear Overhauser effect
OAA	oxaloacetate
PAGE	polyacrylamide gel electrophoresis
PDI	protein disulfide isomerase
PEP	phosphoenolpyruvate
PRK	phosphoribulokinase
SDS	sodium dodecyl phosphate
Tris	tris(hydroxymethyl)aminomethane
Trx	thioredoxin
V_{max}	maximum velocity

CHAPTER 1

INTRODUCTION

Intermediary metabolism is primarily controlled by regulating enzyme activity. One common mode of regulation is allosterism, whereby an inhibitor or activator binds to an enzyme at a location distant from the active site. This mode is primarily used to respond to changes in conditions inside the cell. Enzymes can also be regulated by irreversible covalent modification, such as partial proteolysis. The pancreatic proteases, among other enzymes, are subject to this second mode of regulation. Reversible covalent modification is an additional, and perhaps even more prevalent, mode of regulation and includes the commonly known reaction of phosphorylation which usually occurs in response to extracellular signals such as hormones or growth factors. Reversible alterations of the redox status of enzymes offer yet another avenue for regulation. Representative of this latter mode, several chloroplastic enzymes are regulated by oxidation/reduction of sulfhydryls/disulfides, a process requiring thioredoxin. This thioredoxin-modulated regulation of enzyme activity is the focus of the research presented herein.

THE THIOREDOXIN SUPERFAMILY OF PROTEINS

Thioredoxins are members of a superfamily of proteins characterized by the active site motif CXXC, where "X" is any amino acid. Other prominent members of this superfamily are glutaredoxin, Dsb, and protein disulfide isomerase (PDI). Each of these proteins has its own unique functions in the normal lives of cells. Trx most commonly contains the active site sequence CGPC and functions primarily as a protein disulfide reductase (for review, see Holmgren, 1985). Glutaredoxin, like Trx, is a monomeric protein with a single domain but, unlike Trx, it catalyzes GSH-dependent disulfide

reductions and has an active site of CPYC or CPFC (reviewed in Wells *et al.*, 1993). The dimeric protein PDI contains four domains, two of which are Trx-like (Edman *et al.*, 1985). Through its redox active site of CGHC, the isomerase catalyzes the rapid formation of native disulfide bonds (Chivers *et al.*, 1996; for review see Freedman *et al.*, 1994), is abundant in the lumen of the endoplasmic reticulum of cells that are actively synthesizing disulfide-bonded cell surface and secretory proteins, and is reduced directly by GSH. The Dsb proteins, important in the formation of disulfide bonds in bacteria, are monomeric with two domains, one of which is Trx-like (reviewed by Loferer and Hennecke, 1994). Proteins in the Dsb class contain the redox active site sequence CPHC, CVLC, CGYC, or CVAC.

The diversity in the functions of proteins in the thioredoxin superfamily appears to be due to the naturally-occurring variations of "XX" in the CXXC motif (Chivers *et al.*, 1997). These two intervening residues have a direct impact on the reduction potential of the active site disulfide bond with the thioredoxins (E_0' = -0.27 V for *E. coli* Trx)[1] and glutaredoxins (E_0' = -0.23 V) being highly reducing, PDI having an intermediate reduction potential (-0.18 V), and the Dsb proteins being quite oxidizing (E_0' = -0.09 to -0.11 V). In turn, the pK_a value of the first cysteine in the CXXC motif is believed to be a determinant of the reduction potentials. Specifically, disulfide bonds in members of the thioredoxin superfamily are reduced with greater ease as the pK_a of the first cysteine decreases. The

---

[1]The values of E_0' reflect the reduction potentials relative to the $2H^+ + 2e^- \rightarrow H_2$ half-reaction which is assumed to be -0.414 V at pH 7. A $\Delta E_0'$ of 0.03 V corresponds, at 25°C, to a ten-fold change in the equilibrium constant (Chivers *et al.*, 1997).

buried Asp26 carboxyl of *E. coli* Trx (Asp40 in spinach Trx *f*) and the ε-amino group of Lys57 (Lys70 in spinach Trx *f*) may impact the pK_as of the active site thiols, especially that of the first cysteine in the motif, Cys32 (Dyson *et al.*, 1997).

In addition to containing the CXXC motif, all members of the Trx superfamily are believed to have the thioredoxin protein fold (reviewed in Martin, 1995 and Creighton and Freedman, 1993). This fold can be envisioned as a four-stranded β sheet flanked by three α helices; the N-terminus consists of a β strand-α helix-β strand motif, the C-terminus contains a β strand-β strand-α helix motif, and the two motifs are connected by a loop that incorporates a third helix. The thioredoxin fold is slightly smaller than Trx itself, having one less β strand and one less α helix.

THE THIOREDOXIN FAMILY

Thioredoxins are small proteins (approximately 12 kDa) that are ubiquitous in nature. The active site of this redox protein (WCGPC) is highly conserved, with the only known variations being WCPPC in Trx *h* from *Arabidopsis thaliana* (Rivera-Madrid *et al.*, 1995) and WCAPC found in both thioredoxin C2 of the gram-negative bacterium *Corynebacterium nephridii* (Eklund *et al.*, 1991) and in the thioredoxin of spinach roots (Marcus *et al.*, 1991). Thioredoxins fulfill several functions including facilitating the regeneration of oxidatively damaged proteins, acting as a hydrogen donor for methionine sulfoxide reductase and ribonucleotide reductase, activating the extracellular domain of the interferon-γ receptor and the glucocorticoid receptor, and modulating the DNA binding activity of some transcription factors (e.g., NF-κB and TFIIIC) (for reviews see Besse and Buchanan, 1997 and Holmgren, 1989). In addition, Trx is implicated in intercellular signalling due to the fact that it can be secreted and taken up by a variety of cells.

All thioredoxins, with the exception of those found in the chloroplast of

photosynthetic cells, regulate their target proteins through the NADP/thioredoxin system (recently reviewed in Buchanan *et al.,* 1994a and in Besse and Buchanan, 1997). In this system, electrons flow from NADPH to FAD (a coenzyme associated with NADP-thioredoxin reductase), from FAD to the redox active site of NADP-thioredoxin reductase, and finally to Trx. This generates the reduced form of Trx which is then capable of reducing disulfide bridges in target proteins. The NADP/Trx system is located in multiple cell compartments including, in the case of plants, the cytosol, endoplasmic reticulum, and mitochondria.

In a few organisms, several thioredoxins are known to exist. Three types of thioredoxins (designated Trx *h*, *f*, and *m*) are found in photosynthetic cells. Thioredoxins in the *h*-class are located in the cytosol, mitochondria, and endoplasmic reticulum, while the *f* and *m* types are chloroplastic proteins. Recent studies suggest that Trx *h* acts as an early signal in germination (reviewed in Besse and Buchanan, 1997). The targets of Trx *h* include various seed storage proteins (e.g., gliadins and glutenins), enzymes (e.g., thiocalsin, a serine protease which catalyzes the degradation of reduced gliadins and glutenins), and enzyme inhibitors (e.g., α-amylase/subtilisin inhibitor). Five different thioredoxins belonging to the *h*-class have been identified in *Arabidopsis thaliana* (Rivera-Madrid *et al.,* 1995) and two have been identified in spinach (Marcus *et al.,* 1991). Whether or not these different thioredoxins have different functions awaits determination. Interestingly, two thioredoxins have been identified in the rat with one of the two being located exclusively in the mitochondria (Spyrou *et al.,* 1997). In addition, multiple thioredoxins (three in each case) have been reported in the lower eukaryote *Dictyostelium discoideum* (Wetterauer *et al.,* 1992) and in *Corynebacterium nephridii* (Lim *et al.,* 1996). Detailed functional analyses and localization studies are still needed in these cases as well. The role of the chloroplastic thioredoxins will be discussed in detail in the next section of this chapter.

Three-dimensional structures of several thioredoxins have been determined by X-ray crystallography and NMR studies and include those of the oxidized and reduced forms of *E. coli* (Jeng *et al.*, 1994; Dyson *et al.*, 1990; Katti *et al.*, 1990) and human Trx (Qin *et al.*, 1994; Weichsel *et al.*, 1996), oxidized Trx *h* from the eukaryotic green alga *Chlamydomonas reinhardtii* (Mittard *et al.*, 1997), and oxidized Trx-2 from the cyanobacterium *Anabaena* sp. strain PCC7120 (a Trx with *f*-like activities) (Saarinen *et al.*, 1995). The backbones of the reduced and oxidized forms of Trx within and between species are nearly identical and the side chains are packed within the protein core in an extremely similar manner. Conformational differences between the oxidized and reduced structures appear subtle in nature and localized to areas in spatial proximity to the redox active site. One significant difference that does exist between species, however, involves the distance between the S_γ atoms of the redox active cysteines. In the reduced form of human Trx this distance is 3.1 Å (Qin *et al.*, 1994) while in *E. coli* Trx it is 3.8 Å (Jeng *et al.*, 1994). In the latter case, this distance is slightly greater than the sum of the van der Waal radii of the sulfur atoms (2 x 1.85 = 3.70 Å). The distance between the S_γ atoms in the oxidized protein from both species is, however, essentially identical (~2.0 Å). Jeng and colleagues (1994) have pointed out that the high degree of similarity in the structures of Trx in its two redox states allows one to assume that the conversion from one redox state to another requires little energy.

THE CHLOROPLASTIC THIOREDOXINS

Since the discovery of the chloroplastic thioredoxins by Buchanan and colleagues (Wolosiuk *et al.*, 1979), the two different chloroplastic thioredoxins have been perceived as having different target enzyme selectivities. Trx *f* has appeared to preferentially regulate fructose-1,6-bisphosphatase (FBPase), phosphoribulokinase (PRK), NADP-dependent

glyceraldehyde-3-phosphate dehydrogenase, and sedoheptulose-1,7-bisphosphatase. Trx *m*, on the other hand, has been believed to preferentially regulate NADP-dependent malate dehydrogenase (MDH) and glucose-6-phosphate dehydrogenase. NADP-dependent glyceraldehyde-3-phosphate dehydrogenase is a member of the reduction phase of the reductive pentose phosphate cycle in which ATP and NADPH (produced in the light reactions of photosynthesis) are consumed in the reduction of 3-phosphoglycerate to glyceraldehyde 3-phosphate. FBPase, PRK, and sedoheptulose-1,7-bisphosphatase are involved in the regeneration phase of the reductive pentose phosphate cycle in which glyceraldehyde 3-phosphate is converted to the CO_2 acceptor, ribulose 1,5-bisphosphate. Glucose-6-phosphate dehydrogenase and MDH are unique among the targets of the chloroplastic thioredoxins in that they are not members of the reductive pentose phosphate cycle. Glucose-6-phosphate dehydrogenase catalyzes the first step in the oxidative pentose phosphate pathway, the alternative to glycolysis for carbohydrate degradation. The primary function of this enzyme is to provide NADPH for maintaining the biosynthetic reactions of photosynthesis in the dark. MDH will be discussed in the next section. An additional target of the chloroplastic thioredoxins is ATP synthase (CF_1-ATPase), an enzyme involved in photophosphorylation. Both Trx *f* and *m* can activate this target, although Trx *m* is claimed to be superior (McKinney *et al.*, 1979).

The chloroplastic thioredoxins regulate their target enzymes through the ferredoxin/thioredoxin system (Fig. 1-1)[2] (reviewed in Buchanan, 1984; Buchanan, 1986; Buchanan *et al.*, 1994a; Buchanan *et al.*, 1994b; Buchanan, 1991; and Scheibe, 1990). This system, composed of ferredoxin, ferredoxin-thioredoxin reductase (FTR), and Trx, operates as follows: The electron transport system of photosystem I of illuminated

[2]All figures and tables may be found in the Appendix.

chloroplasts reduces ferredoxin. Electrons are then transferred from reduced ferredoxin to Trx through the action of the iron-sulfur enzyme FTR. Consequently, reduced Trx is generated which can then reduce its target enzymes. (In *in vitro* assays, FTR is routinely substituted with dithiothreitol.) This directional electron flow relaxes in the dark resulting in the reoxidation of target enzymes (Gilbert *et al.*, 1990). The *in vivo* oxidant is assumed to be Trx (Buchanan, 1992; Buchanan *et al.*, 1994a; Leegood and Walker, 1980; Scheibe, 1981), although direct, conclusive evidence of its identity or even the necessity for a specific oxidant is lacking. Biosynthetic enzymes, including members of the Calvin cycle, are activated by light, whereas degradative enzymes are deactivated. Thus, all of the target enzymes of Trx *f* and *m* become catalytically active upon reduction by Trx, with the exception of glucose-6-phosphate dehydrogenase which is deactivated by reduction. Thus, a futile cycle of glucose synthesis in the reductive pentose phosphate pathway and glucose catabolism in the oxidative pentose phosphate pathway is prevented. In essence, then, the ferredoxin/thioredoxin system minimizes the simultaneous functioning of opposing metabolic pathways and maximizes the efficiency of each pathway (Buchanan 1980).

Reduction of the target enzymes by thioredoxin occurs through thiol-disulfide exchange (Fig. 1-2). A thiolate of Trx attacks the disulfide bond on the target protein in the first step of this pathway, forming a protein-protein mixed disulfide intermediate. A second thiolate of the complexed Trx then intramolecularly attacks the mixed disulfide, generating reduced target enzyme and oxidized Trx. Through site-directed mutagenesis, the primary nucleophile that attacks the disulfide of target proteins has been identified (Brandes *et al.*, 1993). Each of the two redox active cysteines of spinach Trx *f* were independently substituted with serine and the resulting mutant proteins were analyzed for their ability to activate oxidized spinach FBPase in the presence of DTT. Mutation of Cys46 eliminated the thioredoxin's ability to activate the target, whereas the C49S mutant protein was still capable of this function. Thus, Cys46 is the primary nucleophile of Trx *f*

and Cys49 serves to cleave the mixed disulfide intermediate. This finding is compatible with three-dimensional structure information on *E. coli* Trx which indicates that Cys32 (Cys46 in spinach *f*), but not Cys35 (Cys49 in spinach *f*), is solvent accessible (Katti *et al.*, 1990).

The rate constants for the intermolecular and intramolecular steps of thiol-disulfide exchange are influenced by thiol pK_a, binding interactions, steric effects, and local charge (for a review of thiol-disulfide exchange, see Gilbert, 1990 and Gilbert, 1995). The dominant forces which influence the intramolecular steps, however, are strain and entropy. Many of these effects can be quite large, with the rate constant for the reaction of a thiolate anion with a disulfide, for instance, decreasing by a factor of 3.2 for each unit decrease in the pK_a of the attacking thiolate.

The equilibrium constants for thiol-disulfide exchange are influenced by the same factors as the rate constants. The equilibrium constant (K_{ox}) for the oxidation of Trx is represented by the equation $K_{ox} = [\text{Trx-S}_2][\text{target-SH}_2] / [\text{Trx-SH}_2][\text{target-S}_2]$ if mixed disulfide intermediates are neglected. This indicates, then, that at equilibrium the ratio of reduced to oxidized target enzyme and, therefore, the level of target enzyme activity, is directly related to the ratio of oxidized to reduced Trx and the equilibrium constant. High K_{ox} values indicate a stable intramolecular disulfide bond. K_{ox} values for the reaction of the chloroplastic thioredoxins with GSSG have been determined to be approximately 1000 M. For comparison, DTT, also in a reaction with GSSG, has a K_{ox} value of 10,000 M. K_{ox} values for FBPase, on the other hand, range from 1200 M to 4000 M and the reported value for MDH is 4400 M.

The reduction potential of the half-reaction

$$\text{target-S}_2 + 2H^+ + 2e^- \rightarrow \text{target-(SH)}_2$$

is given by the Nernst equation: $E = E_0 - (RT / nF) \ln [\text{target-}(SH)_2] / [\text{target-}S_2][H^+]^2$, where E_0 is the standard reduction potential (i.e., the reduction potential at the standard state of $[\text{target-}(SH)_2] = [\text{target-}S_2] = [H^+] = 1$ M), F is Faraday's constant, n is the number of electrons, T indicates the temperature, and R is the gas constant. A similar equation can be written for thioredoxin. Many of the reported values for the reduction potentials of the thioredoxins and target enzymes are actually based on the use of a standard reduction potential of -0.32 V at pH 7.0 and 25°C for NADPH and an equilibrium constant for the glutathione reductase reaction of 100 M. Using this approach, the reduction potentials of FBPase and MDH were determined to be identical (-0.37 V) and similar to those of the chloroplastic thioredoxins (-0.35 V).

TARGET ENZYMES OF THE CHLOROPLASTIC THIOREDOXINS

The primary focus of this dissertation research concerns the thioredoxin-mediated regulation of three chloroplastic enzymes: FBPase, MDH, and PRK.

Fructose-1,6-Bisphosphatase

FBPase catalyzes the hydrolysis of fructose 1,6-bisphosphate to fructose 6-phosphate using Mg^{2+} as a cofactor. Several biochemical characteristics of the enzyme have been determined. Each subunit of this enzyme is 40-45 kDa, with a tetramer existing at physiological pH (7-8) (Zimmerman *et al.*, 1976; Nishizawa and Buchanan, 1981). The tetramer readily dissociates to a dimeric form at pH 8.8, causing a decline in specific activity. Charles and Halliwell (1980) have reported that, upon reduction of the disulfide(s), the K_m for FBP decreases from 800 to 30 μM and the K_m for Mg^{2+} is reduced

from 900 to 200 μM. By monitoring the binding of ^{125}I-labeled Trx *f* to FBPase at pH 7.5, Soulie and colleagues (1985) have determined a K_d value of 0.8 μM. In addition, kinetically saturating concentrations of FBP do not alter the affinity of Trx for FBPase. Thus, the active site and Trx-binding site of this enzyme are believed to be distinct (Soulie *et al.*, 1985).

Amino acid sequences have been determined for FBPase from several chloroplastic and nonchloroplastic sources. Spinach chloroplastic FBPase is approximately 80% homologous to the wheat chloroplastic enzyme but only 40% homologous to the FBPases of mammals, yeast, and *E. coli*. Amino acid sequence alignments clearly show that the chloroplastic form of this enzyme contains an insertion of approximately 12-17 residues relative to the nonchloroplastic forms (Marcus *et al.*, 1988; Marcus and Harrsch, 1990; Jacquot *et al.*, 1995). The insertion is located near the center of the primary structure and, interestingly, contains two cysteines separated by only four amino acids: CXVAVC, where X=Val in spinach FBPase and Ile in the soybean, pea, wheat, *Arabidopsis thaliana*, potato, and rapeseed enzymes. Consequently, this insertion may be important in light-dependent activation (Marcus and Harrsch, 1990).

Immediately preceding this unique insertion is an amino acid segment (Pro151-Ser168 [3]), which is poorly conserved. Hermoso *et al.* (1996) have expressed this region of the pea chloroplastic enzyme as a fusion protein in *E. coli*. Through ELISA and gel filtration studies, the authors have demonstrated that this segment "strongly" interacts with pea Trx *m*. Supportive of this result, the crystal structure of spinach chloroplastic FBPase (Villeret *et al.*, 1995) shows that this segment is part of a protruding loop that appears on

---

[3]Throughout this dissertation, all references to amino acid residues correspond to those found in the spinach proteins, except where indicated.

all four subunits of the tetrameric enzyme, thereby making the segment accessible to Trx.

Spinach chloroplastic FBPase contains seven cysteinyl residues per subunit (residues 51, 94, 155, 174, 179, 191, and 307), four of which are unique to the chloroplastic FBPases (94, 155, 174, and 179). The number of accessible sulfhydryl groups and disulfide bridges has been examined by reactions with the thiol-specific reagent 5,5'-dithiobis-(2-nitrobenzoic acid) (DTNB) (Pradel *et al.*, 1981). The oxidized, homotetrameric form of the enzyme contains six disulfide bridges and 12 unaccessible sulfhydryl groups at pH 7.5. In contrast, upon reduction by DTT, the tetrameric form has four disulfide bridges and eight unaccessible groups. Thus, the authors concluded that activation of FBPase involves the reduction of two disulfide bridges. Aragnol and colleagues (1985), using the same reagent, also concluded that two disulfide bridges are reduced upon activation. A more recent study involving titration of sulfhydryls of FBPase with DTNB indicates, however, that only one regulatory disulfide bridge exists per subunit (Chen and Xu, 1996). The two studies also contradict each other with respect to the existence of accessible thiols in the oxidized form of FBPase. While the earlier report claims that this form of the enzyme lacks accessible thiols, the more recent study reports that four accessible sulfhydryls exist. Modification of the first two with DTNB had only a minor impact on activity, while modification of the remaining two caused a dramatic reduction in activity.

Although the crystallographic structure (2.8 Å resolution) of oxidized spinach chloroplastic FBPase has been solved (Villeret *et al.*, 1995), it does not, unfortunately, provide definitive information regarding the identity of the regulatory cysteines in this enzyme. The crystallographers report that neither Cys94 nor Cys307 has another cysteine in close enough proximity with which it could form a disulfide bond. The distance between the S_γ atoms of cysteines 155 and 174 or 179 is 7-18 Å (depending upon which

subunit of the tetramer is examined), while this distance between residues 174 and 179 (the two cysteines in the unique chloroplastic insertion) varies from 5-16 Å. The crystallographers claim that a disulfide bridge between residues 174 and 179 could only form if a large conformational change occurs. Cysteines 51 and 191 are closer to each other (3.9-4.6 Å), making it possible for them to form a bridge. In addition, the authors (Villeret *et al.,* 1995) mention that if the S_γ atom is rotated around the χ^1 torsion angle of Cys51, the distance between the S_γ atoms decreases even further to 2.4-2.7 Å, thereby making disulfide bridge formation even more likely. In addition, a modeling study based upon the structure of pig kidney FBPase claimed that cysteines 51 and 191 are capable of forming a disulfide bridge (Li *et al.,* 1994). In the crystallographic structure of spinach FBPase, however, a density corresponding to a bridge was not observed.

Site-directed mutagenesis studies have been used to attempt to identify the regulatory sulfhydryls of chloroplastic FBPase. Mutagenesis of this enzyme from pea was used by Jacquot and colleagues (1995) to generate the double mutant C174S/C179S, thereby substituting both cysteines in the unique chloroplastic insertion. The authors report that the mutant protein was permanently active and insensitive to thiol agents (including Trx). The conclusions from their study indicate that either one or both of these residues is normally involved in a disulfide bridge, though not necessarily with each other. The same laboratory in a later study (Jacquot *et al.,* 1997) reported the preparation of single cysteine to serine mutants involving residues 51, 155, 174, 179, and 191. The C155S mutant was permanently active and redox independent, contrary to the C191S and C51S mutants. Mutations at positions 174 and 179 also affected the redox properties of the enzyme (causing it to be partially deregulated), although not to the extent of the C155S mutation. The authors concluded that Cys155 in pea FBPase is clearly regulatory. Jacquot and colleagues (1997) have proposed that Cys155 is bridged alternately with Cys174 and

Cys179, with a total of only one regulatory disulfide bridge existing in the enzyme at any given time.

In agreement with Jacquot and colleagues (1997), site-directed mutagenesis at positions 51, 94, 155, 174, 179, 191, and 307 in FBPase from rapeseed (*Brassica napus*) showed that Cys155 contains a regulatory sulfhydryl (Rodriguez-Suarez *et al.*, 1997). In addition, Cys174 and Cys179 were implicated as having a role in reductive activation. However, it was not possible to elucidate the exact pairing(s) involved in the disulfide bridge(s) from these studies (Rodriguez-Suarez *et al.*, 1997).

In summary, despite extensive study by many laboratories, the number of regulatory disulfides in FBPase as well as their identity remain uncertain. Among all the contradictory results, the possibility remains that the two proximal cysteines in the unique amino acid insertion are regulatory. Whether these two residues form a disulfide bridge with each other or additional regulatory cysteines exist awaits determination.

NADP-Dependent Malate Dehydrogenase

The NADP-dependent form of malate dehydrogenase, located only in chloroplasts, is metabolically important in both C3 and C4 plants, although it is involved in a different pathway in each case (reviewed in Gietl, 1992). In C3 plants (e.g., spinach, pea, and wheat), the initial reaction in the fixation of atmospheric carbon dioxide is catalyzed by ribulose-1,5-bisphosphate carboxylase, whereby ribulose-1,5-bisphosphate is converted to two molecules of 3-phosphoglycerate in the first step of the reductive pentose phosphate pathway. Contrary to C3 plants, C4 plants are specialized in limiting the loss of assimilates by photorespiration. The primary carboxylation reaction in all C4 plants is that which is catalyzed by phosphoenolpyruvate carboxylase (i.e., the conversion of phosphoenolpyruvate to oxaloacetate) in the cytoplasm of mesophyll cells. The most common type of C4 plant and the only type in which NADP-dependent malate

dehydrogenase has a major role is that of the NADP-malic enzyme type (e.g., sorghum, maize, and ice plant). The essential role of MDH in C3 plants is in balancing reducing equivalents (ATP and NADPH) between the chloroplast and cytosol via the malate/oxaloacetate shuttle. In this shuttle, malate produced from the reduction of oxaloacetate (OAA) as catalyzed by MDH, is readily transported across the chloroplast membranes into the cytosol. Once in the cytosol, the malate is oxidized to OAA by NAD-dependent malate dehydrogenase with the concomitant production of NAD. OAA then proceeds back into the chloroplast stroma to reinitiate the cycle. This shuttle is presumably essential because of the impermeability of the chloroplast membranes to NADP(H) and NAD(H). C4 plants of the NADP-malic enzyme type use MDH to convert OAA to malate in the chloroplasts of mesophyll cells. The malate is subsequently shuttled to the chloroplasts in neighboring bundle sheath cells where it becomes decarboxylated by NADP-malic enzyme to form pyruvate. In this reaction, the NADPH that is formed is used in the reductive pentose phosphate pathway. The pyruvate, meanwhile, is returned to the mesophyll cells and phosphorylated to PEP, allowing the cycle to reinitiate. Despite these different reasons for needing MDH, this enzyme is regulated by the ferredoxin/thioredoxin system in both C3 and C4 plants. NAD-dependent malate dehydrogenase, whether located in the mitochondria or cytoplasm of higher plants, in mammalian cells, or bacterial cells, is not regulated by its redox status.

Each subunit of MDH has a molecular weight of approximately 40 kDa. The usual physiological state for MDH is a dimer, independent of redox status. Amino acid sequences of the NADP-dependent forms of MDH are approximately 85% identical. Their similarity to the NAD-dependent enzyme from the bacteria and cytosol is only 40-50%. Amino acid sequence similarity between the chloroplastic and mitochondrial malate dehydrogenases is lowest, with a value of only 20%. All known chloroplastic malate dehydrogenases have two amino acid extensions relative to the NAD-dependent isoforms:

(1) a 45-amino-acid extension exists at the amino terminus which contains two cysteines and (2) a 15-residue extension is present at the carboxy terminus containing one cysteine. The uniqueness of these extensions has led researchers to propose that they are important for regulation by Trx. The five cysteinyl residues located between the extensions in all NADP-dependent malate dehydrogenases are not found at the corresponding positions in NAD-dependent MDHs.

The following site-directed mutants of sorghum NADP-MDH have been generated to ascertain whether the amino terminus of the enzyme contains a regulatory disulfide bridge: C24S, C29S, C24S/C29S, and a truncation mutant which lacks the extended amino terminus present in the chloroplastic malate dehydrogenases (Issakidis *et al.*, 1992). The authors reported that all mutants were activated by Trx *m* more rapidly than wild-type, and they reached the conclusion (perhaps erroneously) that since both the single and double mutants were similar, cysteines 24 and 29 form a disulfide bridge with each other. A triple cysteine mutant was subsequently generated in which the cysteine immediately preceding the C-terminal extension (Cys365) as well as the two cysteines in the amino terminal extension (24 and 29) were converted to alanine (Issakidis *et al.*, 1993). The activity of the mutant protein was not enhanced by preincubation with reduced Trx or DTT, implicating Cys365 as an additional regulatory site.

Additional site-directed mutagenesis studies with the sorghum enzyme have been performed with the cysteines in the carboxy-terminal region in an attempt to identify the disulfide bridge pair of Cys365 (Issakidis *et al.*, 1994). Cysteines 365 and 377 were substituted with alanine, either separately or together. The time courses of activation by Trx *m* were similar to wild type in all cases. Contrary to wild-type, the mutant proteins were slightly active in the absence of reductant. Combining these C-terminal mutations with the amino terminal mutations utilized previously (i.e., C24S/C29S/C365A, C24S/C29S/C377A, and C24S/C29S/C365A/C377A) resulted in proteins which were

completely active without pretreatment with DTT or Trx (Issakidis *et al.,* 1994). From these experiments, Issakidis *et al.* (1994) conclude that a second regulatory disulfide bridge exists in MDH, bonding cysteines 365 and 377.

The observation by Issakidis and colleagues that engineered MDH, which lacks the apparent N-terminal disulfide, is rapidly activated while the enzyme that lacks the apparent C-terminal disulfide is as slowly activated as wild-type led to the following tentative model: Reduction of the C-terminal disulfide allows ligand access to the active site, while reduction of the N-terminal disulfide causes a conformational change, allowing the active site to change into its fully active conformation. To test this model, the same laboratory has used the fact that His229 is essential for catalysis and can be specifically derivatized with diethylpyrocarbonate if the MDH is first reduced. The accessibility of the active site was examined, utilizing diethylpyrocarbonate, in two site-directed mutants of MDH: C24S/C29S and C365A/C377A. Supportive of the model, the C365A/C377A mutant was readily derivatized, even in the absence of pretreatment with reductant, while derivatization could only be demonstrated with the C24S/C29S double mutant if the enzyme was first pretreated with reductant (Issakidis *et al.,* 1996).

Additional studies appear to corroborate the role of two disulfide bridges in the production of fully active MDH. In one case, N-terminal truncations of MDH from pea and spinach were generated through digestion with aminopeptidase K, resulting in removal of the two N-terminal cysteines in each case (Ochertina *et al.,* 1993). These shortened forms of the enzyme were still redox sensitive. However, only low concentrations of thiol (40 mM BME) were needed for complete activation. A similar approach has been taken with the C-terminal portion of the enzyme from pea (Fickenscher and Scheibe, 1988). Treatment of the inactive, oxidized enzyme with carboxypeptidase Y resulted in partial activation of the enzyme. Enhancement in activity was observed following incubation with DTT. Other studies have concluded that the two cysteines in the unique N-terminal

extension of MDH (Decottignies *et al.*, 1988; Scheibe *et al.*, 1991) and the two cysteines closest to the C terminus (by modeling, Jackson *et al.*, 1992) form regulatory disulfides. On the contrary, two groups have suggested that one of the two cysteines in the C-terminal region forms a disulfide bridge with an internal cysteine (Reng *et al.*, 1993; Li *et al.*, 1994), but different cysteines are implicated in each of the two cases.

Phosphoribulokinase

PRK, in a homodimeric state, catalyzes the ATP-dependent phosphorylation of D-ribulose 5-phosphate to form D-ribulose-1,5-bisphosphate, the requisite acceptor of CO_2 in photosynthetic carbon fixation. Each 40-kDa subunit of the kinase contains a total of four cysteinyl residues. Contrary to FBPase and MDH, those which are regulatory have been conclusively identified (Porter *et al.*, 1988). Experiments undertaken for this purpose are as follows: Firstly, oxidation of PRK with DTNB demonstrated that the formation of a single intramolecular disulfide bond leads to the complete inactivation of the enzyme. Oxidized PRK was then *S*-carboxymethylated with [^{14}C]iodoacetate under denaturing conditions, dialyzed, digested with trypsin, and subjected to reverse phase HPLC. Two peaks of radioactivity were obtained with this sample, while a comparably treated sample of reduced PRK showed four peaks. Therefore, the two peptides containing the regulatory cysteines had been identified. Following purification of the relevant cysteine-containing peptides and sequencing by Edman degradation, the regulatory cysteinyl residues were directly identified as 16 and 55.

An unusual characteristic of PRK is that both of its regulatory cysteines are located in the ATP-binding domain (Porter and Hartman, 1986; Porter *et al.*, 1990). While Cys16 lacks a catalytic function, Cys55 has a modest catalytic role (Brandes *et al.*, 1996b; Milanez *et al.*, 1991; Porter and Hartman, 1988). Cross-linking studies have indicated that a

contributing factor to oxidative deactivation of PRK is the presence of conformational restraints imposed by the disulfide bond (Brandes *et al.*, 1992).

A stable covalent complex has been formed between PRK and Trx *f* by incubating a C16S mutant of spinach PRK with a C49S mutant of spinach Trx *f* in the presence of the oxidant Cu^{2+} (Brandes *et al.*, 1996a). Under the same experimental conditions, a complex could not be formed between C16S PRK/C46S Trx, C55S PRK/C46S Trx, or C55S PRK/C49S Trx. Thus, Cys55 of spinach PRK forms a protein-protein mixed disulfide with Cys46 of spinach Trx *f*.

OBJECTIVE AND APPROACH

Undertaking a study on the regulation of target enzymes of the chloroplastic thioredoxins provides an opportunity to more fully understand carbon flow through the reductive pentose phosphate cycle during carbon dioxide assimilation. Although this study focuses on the chloroplastic thioredoxins, the results should enhance our understanding of the interactions between all other thioredoxins and their specific targets due to the high degree of three-dimensional homology among thioredoxins.

The approach used in this study to more thoroughly elucidate the Trx-modulation of target enzymes involves kinetic analyses of the activation of FBPase, MDH, and PRK by the wild-type chloroplastic thioredoxins and site-directed mutants of Trx *f* designed to be more like Trx *m*. Attempts to develop a strategy for direct quantitation of the binding of the thioredoxins to their targets is also described.

CHAPTER 2

IDENTIFICATION OF RESIDUES OF SPINACH THIOREDOXIN *f* THAT INFLUENCE INTERACTIONS WITH FRUCTOSE-1,6-BISPHOSPHATASE AND NADP-DEPENDENT MALATE DEHYDROGENASE

As the two chloroplastic thioredoxins appear to preferentially activate different target enzymes, an understanding of the thioredoxin-modulated regulation of the targets can be obtained by elucidating binding and selectivity determinants of the Trx. As one approach to this issue, the roles of residues that appear unique to Trx *f* relative to other thioredoxins were explored by site-directed mutagenesis. One such residue is Lys58 which is replaced by glutamate in spinach Trx *m*, *E. coli* Trx, and indeed the majority of thioredoxins in other organisms (Fig. 2-1A) (Eklund *et al.*, 1991). Based on the structure of *E. coli* Trx (Dyson *et al.*, 1990; Katti *et al.*, 1990; Jeng *et al.*, 1994), Lys58 is positioned on the surface (residue 44 in Fig. 2-2), is salt-bridged with residue 110 (Asp in Trx *f*; Lys in *E. coli* Trx and Trx *m*), and is located near the active site. Hence, the K58E mutant of Trx *f* was constructed and characterized.

Residues 74, 75, and 77 were also examined. These residues are located near a conserved, putative hydrophobic contact surface encompassing Gly33, Pro34, Ile75, Pro76, Val91, Gly92, and Ala93 of *E. coli* Trx (Eklund *et al.*, 1991; Xia *et al.*, 1992; Holmgren 1985). Specifically, the region of 74-77 appears to be on the same general face of the molecule as both the hydrophobic contact site and the active site (based upon visual inspection of the *E. coli* Trx structures reported by Dyson *et al.*, (1990) and Katti *et al.*, (1990)). One sequence alignment (de Lamotte-Guery *et al.*, 1991; Wedel *et al.*, 1992) (Fig. 2-1B) suggests that the Asn74 of Trx *f* aligns with an Asp in Trx *m* and Asp61 of *E. coli* Trx, resulting in an insertion of an asparagine at position 77. Supportive of this

alignment, a D61N *E. coli* Trx mutant generated by Jacquot and colleagues showed an increase in efficiency of spinach FBPase activation (de Lamotte-Guery *et al.,* 1991). An alternative sequence alignment (Eklund *et al.,* 1991), however, indicates that Asn74 represents an insertion, with Gln75 aligning with aspartic acid in Trx *m* (Fig. 2-1A). Given this uncertainty, two deletion mutants (ΔN74 and ΔN77), as well as two single-substitution mutants (N74D and Q75D), were constructed. The kinetic parameters of these four mutants and the K58E mutant of Trx *f* in the activation of both FBPase and MDH were determined and compared to the corresponding parameters of wild-type Trx *f* and Trx *m*.

Two additional residues of interest are Val89 and Thr105, both of which are actually part of the putative hydrophobic contact surface (Fig. 2-3). Three-dimensional structures indicate that these two residues are located in loops that oppose the active site (loop 1 includes residues 74-76 in human Trx while loop 2 includes residues 90-92). The formation of a disulfide bond appears to make both the active site and the opposing loops "more rigid" (Qin *et al.,* 1994). The side chains in this region appear to be packed more tightly in the reduced form than in the oxidized form. Also, the structures of *E. coli* Trx seem to indicate that both the side chain and backbone of Ile75 (Val89 in spinach Trx *f*) make contact with the disulfide bond in oxidized Trx, with the C_α of Ile75 swinging away from the position of the double bond in reduced Trx (Jeng *et al.,* 1994). The structural data on human Trx with either one of two of its targets (NFκB and Ref-1) suggest that both residues are available for interaction with target enzymes. Specifically, Thr74 (Val89 in Trx *f*) forms a hydrophobic interaction with Tyr60 of NFκB/Trp67 of Ref-1 and a hydrophobic interaction also exists between Ser90 of human Trx (Thr105 in Trx *f*) and Glu63 of NFκB/Ile64 of Ref-1. In addition, both the backbone amide of Thr74 of human Trx and the hydroxyl of Ser90 are hydrogen bonded to the target (Qin *et al.,* 1995; Qin *et al.,* 1997). The report on the Trx-2 structure of *Anabaena* also proposes Ile75 (Val89 in

Trx *f*) as a contact site based on structural comparisons to other thioredoxins and modelling studies with spinach MDH and FBPase (Saarinen *et al.,* 1995). Thus, the single mutant of T105I and the double mutant V89I/T105I were generated in the present study, with the newly-inserted residues corresponding to those found in Trx *m*. Both mutants were studied in the activation of FBPase.

EXPERIMENTAL PROCEDURES

Materials

Oligonucleotides, with the exception of those for V89I and T105I, were synthesized by phosphoramidite chemistry with an Applied Biosystems model 392 DNA/RNA synthesizer by following the manufacturers instructions. The oligonucleotides for the two remaining site-directed mutations were custom synthesized by Gibco BRL. 5′-[α-^{35}S]dATP (1000 Ci/mmol) was obtained from DuPont New England Nuclear. Bacto-tryptone and bacto-yeast extract were obtained from Difco. DTT, Bicine, HEPES, and Tris (free base) were purchased from Research Organics. Assay coupling enzymes, NAD, NADPH, oxaloacetate, EDTA, and BSA were from Sigma. FBP was from Boehringer Mannheim.

Site-Directed Mutagenesis

Site-directed mutants of spinach Trx *f* were generated according to the procedure of Kunkel (1987) using the plasmid pFL404 (Brandes *et al.,* 1993). Single-stranded dU-substituted template was generated in the *E. coli* strain CJ236 which had been infected with M13K07 helper phage. Oligonucleotide primers used to encode the denoted structural changes are indicated in Table 2-1. The primer extension reaction products were electroporated into competent *E. coli* MV1190 cells with the BioRad Gene Pulser.

Following selection on LB medium containing ampicillin, candidate mutants were screened by dideoxy-terminator cycle sequencing (Sanger *et al.*, 1977) using U.S. Biochemical Corp. Sequenase version 2.0 and instructions therein.

A single colony of *E. coli* strain MV1190, containing the desired expression plasmid, was used to inoculate 20 ml of 2x YT (Sambrook *et al.*, 1989) medium containing 50 μg/ml ampicillin and 1% (v/v) glycerol. By shaking at 37° C overnight, a stationary culture was generated. This culture was then diluted 1:50 into 500 ml of the same medium in a 2-liter baffled flask and shaken at 250 r.p.m. at 37° C for 4 hours (A_{600nm} = 2.3). Isopropylthio-ß-D-galactopyranoside was then added to a final concentration of 100 μM. After shaking for an additional 3 hours, the cells were harvested by centrifugation, washed once with 20 mM Bicine-NaOH (pH 8.0)/1mM EDTA, and stored at -80° C.

Purification of Trx, FBPase, and MDH

Recombinant wild-type Trx *f* and mutants thereof were purified by successive anionic and cationic exchange chromatography as previously described (Brandes *et al.*, 1993). Preparations used in this study approached electrophoretic homogeneity (Fig. 2-4). All thioredoxins (5-10 mg/ml) were stored in 50 mM Bicine-NaOH (pH 8.0)/0.1 mM EDTA/5 mM DTT/20% (v/v) glycerol at -80° C. Chloroplastic spinach FBPase was partially purified according to published procedures (Brandes *et al.*, 1993; Zimmerman *et al.*, 1976; Marcus *et al.*, 1987). Specific activity values indicated that this preparation was 30-50% pure. Purified recombinant spinach Trx *m* and purified recombinant sorghum leaf MDH were gifts of Professor Peter Schürmann (Université de Neuchâtel, Switzerland) and Professor Jean-Pierre Jacquot (Université Paris-Sud, France), respectively.

Activation of FBPase by Trx

Rates of activation of oxidized FBPase (40 μg/ml) as a function of Trx concentration were determined at 25° C in 50 mM HEPES-KOH (pH 7.8)/0.1 mM EDTA/5 mM DTT. Periodically, 40-μl aliquots of the activation mixture were withdrawn and assayed for FBPase activity. Assay solutions (1 ml) consisted of 50 mM HEPES-KOH (pH 7.8)/50 μM EDTA/1 mM $MgSO_4$/4 mM fructose 1,6-bisphosphate/2 units of phosphoglucose isomerase/3 units of glucose-6-phosphate dehydrogenase/1 mM NAD^+. The formation of NADH was followed spectrophotometrically at 340 nm. One unit of FBPase activity is represented by an absorbance change of 6.22 per minute.

Activation of MDH by Trx

Rates of activation of oxidized MDH (2.6 μg/ml) as a function of Trx concentration were determined at 4° C in 100 mM Tris-HCl (pH 7.9)/10 mM DTT/1 mM EDTA/1 mg/ml BSA. At various times, 20-μl aliquots of the activation mixture were removed and assayed for MDH activity. The assays, in a 100 μl volume, were performed at 25° C in 100 mM Tris-HCl (pH 7.9)/1 mM EDTA/1 mg/ml BSA/1.5 mM oxaloacetate/0.3 mM NADPH. The oxidation of NADPH was followed spectrophotometrically at 340 nm. One unit of MDH activity corresponds to an absorbance change of 6.22 per minute. The rates reported are normalized to an assay volume of 1 ml (*i.e.*, the same volume as in the case of the FBPase assays).

RESULTS

Published values for kinetic parameters of activation of FBPase and MDH by Trx *f* or Trx *m* vary widely. Thus, direct determination of the quantitative impact of the

designed structural alterations of Trx *f* required a reexamination of the properties of the wild-type thioredoxins. Consistent with prior reports (Wolosiuk *et al.*, 1979; Häberlein and Vogeler, 1995), wild-type Trx *f* is far superior to wild-type Trx *m* in the activation of FBPase, displaying a 35-fold higher affinity and a 25-fold increased V_{max} (Fig. 2-5 and Table 2-2). All of the mutants analyzed are impaired relative to wild-type Trx *f*, but still superior to Trx *m*, when analyzed with FBPase (Table 2-2). The largest deviation from the $S_{0.5}$ value of 0.9 μM determined with wild-type Trx *f* occurs with the V89I/T105I mutant, in which case the affinity is lowered about 47-fold (Fig. 2-6 and Table 2-2). This affinity is even slightly less than that observed with wild-type Trx *m*. The single substitution of T105I, however, only doubled the $S_{0.5}$ value relative to wild-type Trx *f* (Fig. 2-6 and Table 2-2). Among the mutations generated outside of the putative hydrophobic contact site, the largest deviation from the $S_{0.5}$ value of wild-type Trx *f* exists with the Asn-77 deletion mutant, displaying a 15-fold reduction in affinity. Among the mutants analyzed, replacement of Lys58 by a glutamyl residue has the largest negative impact on V_{max} with a decrease of 3-fold, while the double mutation actually caused a doubling of V_{max}.

As anticipated, Trx *m* is far more effective as an activator for MDH than for FBPase. Indeed, the rates of activation of MDH by Trx *m* are so rapid that reliable monitoring could only be achieved at 4°C as opposed to room temperature. Even without correction for this differential in temperature, the V_{max} for Trx *m* in the activation of MDH is 21 mU/min. (Fig. 2-7) compared to 2 mU/min. in the activation of FBPase (Fig. 2-5 and Table 2-2); however, the $S_{0.5}$ values for the interaction of Trx *m* with the two enzymes are both approximately 30 μM. Despite the efficiency of activation of MDH by Trx *m*, a comparison of the activation profiles for MDH by Trx *f* and Trx *m* argues against preferential regulation by the latter (Fig. 2-7). Even though rate-saturation with respect to

Trx *f* concentrations up to 50 μM cannot be demonstrated, signifying very weak association between Trx *f* and MDH, the rates of activation of MDH by Trx *f* are more rapid than those with Trx *m* throughout the concentration range examined.

The activation kinetics of MDH by the mutants of Trx *f* are complex, exhibiting pronounced sigmoidicity as seen with wild-type Trx *m* (Fig. 2-8). However, analogously to wild-type Trx *f*, the mutants do not show rate saturation in activation of MDH. Thus, the relative effectiveness of Trx *f* mutants as activators of MDH are expressed as apparent second-order rate constants (Table 2-3) calculated from the linear region of the activation curves (Fig. 2-8). Based on this criterion, all mutants are more effective than wild-type Trx *f* in the activation of MDH.

DISCUSSION

Despite both qualitative and quantitative variations among published data, several laboratories have confirmed differential selectivities of Trx *f* and Trx *m* for target enzymes as discovered in pioneering studies by Buchanan and colleagues (Buchanan, 1980; Wolosiuk *et al.*, 1979). As the redox potentials of these two thioredoxins are identical (-210 mV) (Salamon *et al.*, 1995), their selectivities must reflect differential affinities for target enzymes and/or differential propensities for sulfhydryl/disulfide exchanges within the Trx-enzyme complexes. The present study was predicated on the supposition that recognition and selectivity determinants of Trx *f* and Trx *m* could be determined by site-directed mutagenesis as guided by clearly discernable structural differences between the two thioredoxins. Satisfyingly, the residues (Lys 58, Val89, and Thr105) and segment (74–77) of Trx *f* chosen for change are shown to influence its efficiency ($V_{max}/S_{0.5}$) and selectivity in the activation of target enzymes.

The impaired efficiency of K58E, relative to wild-type Trx *f*, in the activation of

FBPase is due primarily to a lower V_{max}, indicative of a slower rate of thiol/disulfide exchange within the productive complex. Slower exchange could reflect misalignment of the exchanging groups or altered pK_a values of the active-site sulfhydryls of Trx *f*. Certainly, the functional group of residue 58 is too far removed, 15–20 Å as extrapolated from the three-dimensional structures of *E. coli* Trx (Dyson *et al.,* 1990; Katti *et al.,* 1990), human Trx (Qin *et al.,* 1994), and *Anabaena* Trx-2 (Saarinen *et al.,* 1995), from the active-site sulfhydryls to directly influence their reactivities. However, either suggested outcome could result from conformational perturbations brought about by the lysyl to glutamyl substitution. Any such perturbations must be slight as judged by the mere 2-fold increase in $S_{0.5}$ for activation of FBPase.

The efficiency of activation of FBPase by Trx *f* is very sensitive to changes in residues at positions 74–77 with greater than 9-fold declines among three of the four mutants examined. In contrast to K58E, these mutants are less efficient than wild-type Trx *f* due primarily to weakened interactions with FBPase as gauged by $S_{0.5}$ values. Therefore, residues 74–77 serve as an important recognition site for target enzymes. The earlier finding that replacement of Asp61 of *E. coli* Trx with Asn as located at the corresponding position-74 in Trx *f* improves the activation parameters with FBPase (de Lamotte-Guery *et al.,* 1991) is consistent with this conclusion. The conclusion is further supported by structural information derived from both human and *Anabaena* Trx. With human Trx, long-range NOE contacts between Ala-29 (Thr43 of spinach Trx *f*) and Asp60 (Asn74 or Gln75 of Trx *f*) and also between Trp31 (Trp45 of Trx *f*) and Asp60 are observed in the reduced but not the oxidized forms of the Trx (Qin *et al.,* 1994). This suggests that localized conformational changes in these regions occur upon binding and subsequent activation of target enzymes. Furthermore, the solution structure of human Trx complexed with a peptide from the transcription factor NFκB shows that the guanidinium

group of Arg57 of NFκB forms a salt bridge with the side-chain carboxylates of Asp58 and Asp61 of the Trx (corresponding to Asp72 and Gln75/Glu76 of Trx *f*) (Qin *et al.*, 1995). Functionally, Trx-2 from *Anabaena* resembles Trx *f* (Gleason, 1992), and its overall three-dimensional structure is very similar to that of *E. coli* Trx (Saarinen *et al.*, 1995). However, the regions that correspond to residues 74/75-87 of Trx *f* differ considerably and thus appear poised structurally for preferential contact with target enzymes. Specifically, Saarinen *et al.* (1995) state that differences in secondary structures of these regions and that amino acid substitutions in the hydrophobic cores are the causes of relative altered positions of these residues.

Whereas all of the engineered structural changes of Trx *f* were counterproductive with respect to activation of FBPase, they were beneficial with respect to activation of MDH, thereby validating the conversion of Trx *f* to a more "*m*-like" thioredoxin. Although V_{max} and $S_{0.5}$ values for the activation of MDH by the Trx mutants could not be determined due to the absence of rate-saturation even at 1000-fold molar excess of the given thioredoxin, the observed activation rates were greater with the mutants than with wild-type Trx *f* at concentrations exceeding 30 μM. The Trx *f* mutants were also more akin to Trx *m* with respect to kinetics of MDH activations, displaying sigmoidicity as opposed to linearity with wild-type Trx *f*.

The reduced apparent affinity values and reduced efficiencies in the activation of FBPase relative to wild-type Trx *f* in the case of the two mutants generated in the putative hydrophobic contact site indicate that Val89 and Thr105 are involved in binding to target enzymes. The observation that the V89I/T105I double mutant has an $S_{0.5}$ exceeding that of wild-type Trx *m* and an efficiency of activation that is reduced 20-fold relative to wild-type Trx *f* is surprising. The substitution of Val for Ile at position 89 is a very conservative mutation and, therefore, it was believed prior to the kinetic studies, that it would have little

impact on binding and selectivity. The kinetic results with the double mutant, however, clearly indicate that a valine at position 89 is crucial for optimal interaction with FBPase. Without the availability of the single V89I mutant, however, it is not possible to determine whether the effects of substitutions at positions 89 and 105 are additive or synergistic.

In addition to identifying functional and selectivity elements of Trx *f*, the present study partially addresses some of the published conflicts about relative target enzyme selectivities of Trx *f* and Trx *m*. Although all accounts agree that Trx *f* is superior to Trx *m* in the activation of FBPase (Wolosiuk *et al.*, 1979; Häberlein and Vogeler, 1995; Nishizawa and Buchanan, 1981), some allege that this enzyme is totally refractive to Trx *m* (Schürmann *et al.*, 1981; Tsugita *et al.*, 1983). Given the inefficiency of Trx *m*, 550-fold lower than that of Trx *f*, in the activation of FBPase, negative reports may merely reflect insufficient concentrations and reaction times.

Beyond these readily reconcilable differences, reports concerning activation of MDH range from a striking preferential effectiveness of Trx *m* (Wolosiuk *et al.*, 1979; Crawford *et al.*, 1986) to superiority of Trx *f* (Schürmann *et al.*, 1981; Hodges *et al.*, 1994) as presented herein. These disparities could be due to differences in conditions for activation or differences in approaches to determining kinetic parameters. Shortly after the discovery of Trx *f* and Trx *m* (Wolosiuk *et al.*, 1979), preferential activation of MDH by the latter was reported to be dependent on the presence of high concentrations of chloride (Crawford *et al.*, 1986). Although stimulation of thioredoxin-dependent activation of MDH by 250 mM NaCl is observed, the impact is similar for both Trx *m* and Trx *f* (data not shown). Thus, methods rather than conditions are the more likely basis of variable results among different laboratories. In most prior publications, the level of activation at a given Trx concentration is based on a single, fixed-time-point assay; the rate of activation is then assumed to be linear throughout the time period selected. Thus, to some extent, equilibria are being determined rather than rates at which equilibria are attained. The kinetic patterns

presently reported are based on true initial rates of activation, whereby an incubation mixture of Trx and target enzyme is sampled repeatedly in order to reveal the linear phase of time-dependent activation. Prior oversights to clearly distinguish rates and equilibria can readily account for the wide range of apparent affinities of spinach Trx *f* for spinach FBPase; *e.g.*, $S_{0.5}$ values of 1.6 nM (Häberlein and Vogeler, 1995), 0.19 μM (Aguilar *et al.*, 1992), and 1 μM (Brandes *et al.*, 1993; de Lamotte-Guery *et al.*, 1991) have been reported. Given this enormous variation of apparent affinities with one enzyme system, reports of inverse selectivities of Trx *f* and Trx *m* are understandable. Although two prior studies include true rates of activation of Trx-regulated enzymes, quantitative comparisons with the data presented here are precluded. One report was restricted to an examination of the Trx *m*/MDH system and did not entail a complete profile of the rate dependence on Trx *m* concentration (Scheibe *et al.*, 1986). In the other report, the activation of FBPase by Trx *f* was examined at molar ratios that gave rise to first-order kinetics with respect to Trx *f* concentration (*i.e.*, absence of rate saturation) (Clancey and Gilbert, 1987).

Based on this new finding of clear-cut kinetic superiority of Trx *f*, relative to Trx *m*, in the *in vitro* activation of MDH, the physiological role of Trx *m* needs to be reassessed. The supposition that Trx *f* preferentially regulates FBPase while Trx *m* preferentially regulates MDH is clearly refuted by the present results.

CHAPTER 3

KINETIC AND MUTATIONAL ANALYSES OF THE REGULATION OF PHOSPHORIBULOKINASE BY THIOREDOXINS

During the course of the study described in Chapter 2, Trx *f* was shown to be kinetically superior to Trx *m* as an activator of both FBPase and MDH. As this unexpected finding seemingly contradicted the dogma regarding target enzyme selectivity and, therefore, the generally accepted explanation for the presence of two chloroplastic thioredoxins (Wolosiuk *et al.,* 1979), it seemed only prudent to extend kinetic analyses to another redox-sensitive enzyme. Accordingly, PRK was selected.

Several observations provide evidence that PRK is indeed redox-regulated by Trx. These include Trx-dependence of light activation of PRK in reconstituted systems (Wolosiuk and Buchanan, 1978; Wolosiuk *et al.,* 1979), correlative increases and decreases in the level of the kinase activity in isolated chloroplasts during successive light-dark cycles (Latzko *et al.,* 1970; Avron and Gibbs, 1974; Champigny and Bismuth, 1976; Fischer and Latzko, 1979; Laing *et al.,* 1981), activation of purified preparations of PRK by Trx, and covalent complexation of Trx with PRK by disulfide bridging of regulatory sulfhydryls (Brandes *et al.,* 1996a). However, the relative kinetic efficiency of Trx *f* and Trx *m* in the activation of purified PRK has not been determined. This chapter describes such a comparison and also the effectiveness of several site-directed mutants of Trx *f*, designed to more closely resemble Trx *m*, as activators of PRK. A potential role for GSH in PRK regulation was also examined.

EXPERIMENTAL PROCEDURES

Materials

The following materials were obtained through their indicated sources: DTNB, Fisher Scientific; DTT and Bicine, Research Organics; and EDTA, BME, GSH, ATP, PEP, NADH, pyruvate kinase, lactate dehydrogenase, ribose 5-phosphate, and phosphoriboisomerase, Sigma. Site-directed mutants of spinach Trx *f* were constructed as described in Chapter 2.

Purification of Thioredoxins and PRK

Recombinant wild-type and mutant forms of Trx *f* were purified to electrophoretic homogeneity and stored as previously described (Chapter 2). Purified recombinant spinach Trx *m* was kindly provided by Professor Peter Schürmann of the Université de Neuchâtel in Switzerland. Fully-activated PRK from fresh spinach purchased from a local supermarket was purified as previously described (Porter *et al.*, 1986; Porter and Hartman, 1988) and stored at -80°C at a concentration of 20 mg/ml. SDS-PAGE analysis indicated that the preparation was homogeneous.

Oxidation of PRK

Prior to oxidation, exogenous thiol was removed from the purified preparation of PRK by gel filtration on a Sephadex G-25 SF HR 10/10 column using 40 mM Bicine-KOH (pH 8.0) containing 0.8 mM EDTA as the equilibration buffer. Oxidation was then performed by treatment with a 20% molar excess of DTNB at 25°C until PRK activity could no longer be detected. The DTNB reaction mixture was then exhaustively dialyzed against 50 mM Bicine-KOH (pH 7.8), 1 mM EDTA, 20% glycerol. Stock solutions of the oxidized kinase were stored at -80°C at a concentration of approximately 5 mg/ml. Prior

to oxidation the PRK had a specific activity of 260 U/mg. Incubation of the dialyzed, oxidized PRK with 50 mM DTT for ≥15 min. resulted in a recovery of 80% of this initial activity value. Previous studies have demonstrated that the loss of kinase activity upon incubation with DTNB is concomitant with the formation of a single disulfide bond per subunit of PRK between cysteines 16 and 55, with no other modifications detected (Porter and Hartman, 1988). Thus, DTNB-oxidized PRK can be regarded as identical to the enzyme present in the dark.

Activation of PRK

PRK (0.08 mg/ml, 2 μM) was activated at 25°C by the indicated concentrations of DTT, BME, GSH or Trx (in the presence of low molecular weight thiol) in a buffer containing 40 mM Bicine-KOH (pH 8.0) and 0.8 mM EDTA. Periodically, aliquots were withdrawn for the determination of kinase activity at 25°C. Assay solutions (1 ml) consisted of 50 mM Bicine-KOH (pH 8.0), 40 mM KCl, 10 mM $MgCl_2$, 1 mM ATP, 3 mM phosphoenolpyruvate, 0.3 mM NADH, 5 units of pyruvate kinase, 6 units of lactate dehydrogenase, and 0.8 mM ribulose 5-phosphate (prepared by incubation of 150 mM ribose 5-phosphate and approximately 2 units of the phosphoriboisomerase at room temperature for 30 min. in 1.3 ml of 50 mM Bicine-KOH pH 8.0/40 mM KCl/10 mM $MgCl_2$; 20 μl of this solution was used per 1 ml assay). The formation of NAD^+ was followed spectrophotometrically at 340 nm. One unit of PRK activity corresponds to an absorbance change of 6.22/min.

RESULTS

Activation of PRK By Low Molecular Weight Thiols

In the studies described in Chapter 2, DTT was used in the Trx-dependent activation of FBPase and MDH in order to maintain the Trx in its reduced form. Since neither of these target enzymes is reduced to any significant degree by DTT, the determination of Trx-dependent rates of activation was fairly straightforward. PRK, however, is known to be readily activated by DTT, although the rate at which this occurs had not been thoroughly examined. Thus, prior to analyses of Trx-dependent activation of PRK, the rate at which DTT activates PRK needed to be rigorously determined. The abilities of BME and GSH to activate PRK were also examined, in an effort to identify a reagent that was unable to activate PRK but was still able to maintain Trx in its reduced state.

An examination of the nonphysiological reductants DTT (Fig. 3-1A) and BME (Fig. 3-1B) shows that both can fully activate PRK, although activation does proceed more slowly with the monothiol. In the DTT concentration range of 1-4 mM, the initial rate of activation is directly proportional to the DTT concentration. GSH (Fig. 3-1C) is also capable of fully activating the kinase, with the rates of activation being similar to those obtained with equivalent concentrations of BME. Since all three thiols examined were capable of activating PRK and, therefore, correction of a background rate would have to be made in the activation studies with Trx irrespective of which thiol was selected, a decision was made to proceed with the determination of Trx-dependent rates of PRK activation in the presence of 4 mM DTT.

Comparative Kinetics of the Activation of PRK by Trx *f* and Trx *m*

In order to determine the dependence of activation rate on the concentration of Trx, molar ratios of [Trx]/[PRK] ≥ 5 were used so that $[Trx]_{free}$ would approximate $[Trx]_{total}$

and activation kinetics would be pseudo-first-order. Estimation of initial rates of activation were based on data collected over the range of 0-30% of the full activation level having been achieved. This range represents the linear phase of the activation curves. The Trx-dependent rate of activation (i.e., the activation rate corrected for the basal rate due to DTT alone) did not vary significantly in the presence of 1-4 mM DTT, thereby verifying that Trx remained fully reduced throughout the course of PRK activation.

Initial rates of activation, extracted from time-courses and corrected for the contribution of DTT, are plotted as a function of Trx *f* concentration in Fig. 3-2A. The Trx-concentration dependence curve exhibits sigmoidicity, as typifies interactions of Trx with target proteins (Schürmann *et al.,* 1981; de Lamotte-Guery *et al.,* 1991; Hatch and Agostino, 1992; Geck *et al.,* 1996), and yields a $S_{0.5}$ of 17 μM and a V_{max} of 7 mU/min. In a kinetic study in which the activation mixture contained a 10-fold lower concentration of oxidized PRK (i.e., 0.2 μM), similar $S_{0.5}$ and V_{max} values were obtained (data not shown). Cooperativity may be the cause of this sigmoidicity since, in all cases, the target proteins are multimeric. In other words, the presence of a reductant at one of the two subunits of PRK may be influencing the binding of a reductant to the second, vacant subunit of the enzyme, perhaps by inducing a conformational change. Despite literature indications to the contrary (Wolosiuk *et al.,* 1979), Trx *m* is modestly more efficient than Trx *f* as an activator of PRK due to a lower $S_{0.5}$ (15 μM) and a higher V_{max} (11 mU/min).

The site-directed mutants of Trx *f*, designed to be more akin to Trx *m*, were also analyzed kinetically in the activation of PRK (Fig. 3-2 B, C, and D and Table 3-1). All of the mutants are somewhat impaired with respect to binding of PRK, as judged by their $S_{0.5}$ values, which range from 1.4-fold to 5-fold greater than that of wild-type Trx *f*. Except for K58E, the mutants display enhanced V_{max} values; with N74D, ΔN74, ΔN77, and T105I

the increased rates of reduction of PRK are counterbalanced by the weakened interactions with PRK, whereby the $V_{max}/S_{0.5}$ values range from 0.4 to 1.6 times that of the wild-type Trx *f* value.

Effectiveness of GSH in PRK Activation

The ability of GSH to fully activate PRK (Fig. 3-1C) along with its natural abundance in the chloroplast (4 mM) (Law *et al.*, 1983) leads one to wonder if GSH has a significant role in activating PRK *in vivo*. To explore this issue, initial rates of activation of PRK by GSH were determined. As shown in figure 3-3, the initial rate of activation of PRK saturates with respect to GSH concentration, displaying a V_{max} of 20 mU/min, a value twice that obtained with the wild-type chloroplastic thioredoxins. Saturation suggests that, as in Trx-mediated reduction of PRK, a complex forms between the activator and the target enzyme. The activation curve, like that found when thioredoxins are the activators, is sigmoidal in nature, giving an $S_{0.5}$ value of 24 mM. Therefore, cooperativity may be functioning here as well.

In chloroplasts, a NADPH-dependent glutathione reductase is present to maintain a high ratio of [GSH]/[GSSG]. Consequently, a subsequent kinetic experiment was performed in which 4 mM DTT was present during the activation to mimic the effect of the reductase (Fig. 3-3). The activation of PRK by GSH in the presence of DTT was hyperbolic, rather than sigmoidal, in nature. This could merely be due to experimental error, as the rates of activation at the lower GSH concentrations have greater standard deviations than the rates at higher concentrations. The apparent affinity (K_m) of GSH for PRK is 5 mM and the V_{max} is 12 mU/min. Both of these values are lower than those obtained in the absence of DTT. The V_{max} values obtained in the presence and absence of

DTT, however, are nearly identical if the rate due to DTT alone is added back to the GSH-dependent rate. Therefore, DTT apparently contributes to the activation of PRK despite the large molar excess of GSH. This scenario is possible if the rate at which DTT forms a complex with PRK is much greater than the rate at which GSH does so. DTT, present at a fixed concentration of 4 mM while the GSH concentration is varied, is apparently sequestering a fixed amount of the PRK, rendering it inaccessible to GSH and reducing the apparent V_{max}. The reduced apparent affinity of GSH for PRK in the absence of DTT may be due to competitive inhibition by GSSG that is formed in the reduction of PRK.

DISCUSSION

A survey of the literature reveals contradictory and incomplete information concerning the ability of low molecular weight thiols (both nonphysiological and physiological) to activate PRK. The results presented in this chapter clearly indicate that GSH is capable of fully activating PRK, an observation which has not previously been reported. This result actually contradicts a report by Clasper *et al.* (1994), in which an overnight incubation of PRK with 56 mM GSH did not result in complete reduction of the kinase. In Clasper's study, the apparent inability of GSH to fully reduce the PRK may simply be due to extensive air oxidation of the reductant during the lengthy incubation period. If the authors would have examined earlier time points, perhaps a point at which full reduction had occurred would have been observed. Wolosiuk *et al.* (1985) report that BME is unable to activate PRK (except in the presence of ethanol), whereas the experimental results presented herein demonstrate that BME cannot only activate PRK but can do so completely (that is, high concentrations of BME drive the equilibrium in favor of reduced PRK to completion). In the 1985 study, insufficient reductant concentrations and/or incubation times appear to have been used. Specifically, their activation conditions

involved an incubation of PRK with 10 mM BME for only 5 min. at 23°C. The rapid, complete reduction of PRK by DTT observed in the present study is in agreement with all earlier reports with the exception of one by Rault *et al.* (1991) (in their study, PRK could not be fully activated in the absence of Trx). This chapter, however, provides the first examination of the level of PRK activity following incubation with several different DTT concentrations for several different periods of time.

The fact that the apparent affinity value for GSH and PRK, either in the presence or absence of DTT, exceeds the known *in vivo* concentration of GSH indicates that GSH does not likely function as the *in vivo* regulator of PRK. This result is not entirely surprising since it is known that glutathione reductase is highly active in both light and dark and, therefore glutathione is preferentially maintained in its reduced state at all time (in light, the [GSH] = 4.2 mM, [GSSG] = 0.3 mM; in dark, [GSH] = 3.3 mM, [GSSG] = 0.1 mM; the difference in total glutathione concentration under each condition is statistically insignificant) (Law *et al.,* 1983). GSH would consequently maintain PRK in its reduced state in the dark as well as the light, which is known not to be the case. GSH is also unlikely to function in a Trx-dependent reduction of PRK since GSH is incapable of maintaining Trx in its reduced form (at a [GSH] / [GSSG] ratio of 400, 5 M GSH would be needed to maintain half of the total Trx in its reduced form) (Gilbert, 1990).

An affinity of spinach Trx *f* for spinach PRK has been reported by Rault *et al.* (1991) as 0.8 μM, a value more than 20 times less than that observed in the present study. This low value, however, is inconsistent with their data. In the earlier study the apparent affinity was calculated from variations in the extent of maximal PRK activity (i.e., data obtained after equilibria had been attained). If one uses, instead, their initial rate data on the activation of PRK to estimate the apparent affinity it becomes obvious that the apparent affinity is much greater than 0.8 μM. In addition, close analysis of their time-course data

on the activation of PRK reveals initial rates of activation that are similar to those obtained herein.

Although a slight superiority of Trx *m* in the activation of PRK is observed, the differential in efficiency between activation by wild-type Trx *m* and *f* is small compared to that found in the activation of FBPase by the same proteins. While a two-fold difference in efficiency exists when PRK is the target enzyme (Table 3-1), wild-type Trx *f* is more than 500 times as efficient as Trx *m* at activating FBPase (Table 2-2). This small differential as well as this potential role for Trx *m* in activating PRK *in vivo* contradicts the report by Wolosiuk and colleagues (1979) published at the time of discovery of the two chloroplastic thioredoxins.

This discrepancy has two possible explanations. Firstly, the early conclusions regarding selectivity were based upon an examination of relative activities of PRK following incubation with the individual thioredoxins for a fixed time point. On the contrary, initial rates of activation of the kinase were determined in this research. As discussed in Chapter 2, this approach allows one to avoid the potentially erroneous assumption that the rate of activation is linear during the time period selected. The second possibility for the discrepancy involves the fact that the PRK activated in the 1979 study was not a pure form of the enzyme. Instead, a "regulatory form" was used, described as a PRK-GAPDH "complex". The issue of PRK existing in a complex, as well as the physiological significance of a putative complex, is controversial (for review, see Romanova and Pavlovets, 1997). Several laboratories have reported that PRK exists in a complex. However, most of the reports disagree upon its composition. Specifically, in addition to PRK-GAPDH complex, the following complexes have been described: PRK and Rubisco (Sainis *et al.*, 1989); PRK with Rubisco and phosphoriboisomerase (Sainis *et al.*, 1986); PRK, phosphoriboisomerase, Rubisco, and GAPDH (Rault *et al.*, 1993); PRK, phosphoriboisomerase, Rubisco, GAPDH, sedoheptulose-1,7-bisphosphatase, and

ferredoxin-NADP reductase (Süss *et al.*, 1993); PRK, phosphoriboisomerase, Rubisco, GAPDH, and phosphoglycerate kinase (Gontero *et al.*, 1988). Many of these putative multienzyme complexes may be artifacts of the isolation procedures. In some of the complexes just described, the enzymes in the putative complexes catalyze sequential reactions. This observation does offer some support for PRK existing and functioning in a complex existence and function *in vivo* since, in those instances, it can be argued that the complexes exist to allow for direct channeling of the product of the previous enzymatic reaction to the enzyme catalyzing the subsequent step, thereby offering a kinetic advantage compared to the free forms of the enzymes. However, even in some cases where enzymes of successive reactions are members of a reported complex, the quaternary structures of these enzymes in the complex are different from those of the free enzymes. Rault *et al.* (1993), for example, report that Rubisco exists in a L_2S_4 form in their complex rather than the usual L_8S_8 form. The fact that a preliminary crystal structure of a multienzyme complex from spinach leaves containing PRK, Rubisco, phosphoriboisomerase, and the substrate for Rubisco, ribulose-1,5-bisphosphate, has been reported, however, offers additional support for existence of a true complex (Hosur *et al.*, 1993). Also supportive of multienzyme complex existence is a study in which stromal extracts from spinach were subjected to gel filtration and anion exchange chromatography, followed by limited digestion with trypsin (Süss *et al.*, 1993). This approach is based upon the observation that lysine and arginine residues are commonly part of oligomeric protein interfaces. The authors, therefore, assumed that peptide bonds formed with these residues should be digestible by trypsin upon dissociation of the protein components. In essence, then, any differences in the generation of tryptic peptides between the purified enzymes and the enzymes in the putative complex are presumably caused by protein-protein interactions. While free PRK was readily cleaved by trypsin, PRK in the complex was resistant to

digestion.

Comparative kinetic studies in which the ability of both Trx *f* and *m* to activate free PRK *vs.* PRK in a complex has not been examined heretofore. However, two reports from one laboratory have described the activation of PRK in a complex from spinach (the five-enzyme complex described above consisting of PRK, phosphoriboisomerase, Rubisco, GAPDH, and phosphoglycerate kinase) and in the free state by Trx *f* (Rault *et al.*, 1991; Gontero *et al.*, 1993). They report that activation by either DTT alone or DTT in the presence of spinach Trx *f* occurred more rapidly when the PRK was part of a complex. In addition, the V_{max} of the free form of PRK was less than that observed when PRK was in a complex (Rault *et al.*, 1991). This group also reported that the affinity of Trx *f* for PRK in the complex (K_d = 1.10 x 10^{-7} M) was greater than that for the free form of PRK (K_d = 8.19 x 10^{-7} M). Three possible explanations were offered for these kinetic differences: (1) Cys16 of PRK is more accessible to the Trx when the kinase is in a complex; (2) the aggregation state of PRK impacts interactions between Trx and this target enzyme; and (3) the reduction of PRK is more favorable when the other members of the complex are present. However, a serious complication in these and other studies regarding multienzyme complexes is the fact that the complexes depolymerize in the presence of DTT. Therefore, it seems likely that at least a portion of the PRK that is being activated by Trx in these *in vitro* studies is not actually in a complex. Nonetheless, the reports just described suggest that, quantitatively, different results may have been obtained in this current study if PRK in a complex had been used in the activation experiments. Since comparative, thorough kinetic studies involving Trx *m* have not been performed, however, it is unknown as to whether Trx *f* is superior to Trx *m* in the activation of PRK in a complex state. Hence, such a study is currently being planned. An attempt to form a PRK-Rubisco complex *in vitro* will be made and, if successful, this complex will be utilized in initial rate

studies with wild-type Trx *f* and *m*.

Site-directed mutations in Trx *f* produced unexpected results, with all of the mutants (except for K58E) demonstrating Trx *m*-like characteristics with respect to the rate of thiol-disulfide exchange but Trx *f*-like characteristics with respect to binding. These increased rates of thiol-disulfide exchange could be due to an optimized alignment of the exchanging groups or changes in the pK_a values of the active site sulfhydryls of the thioredoxins. The increase in the $S_{0.5}$ values caused by mutation of residues 74, 75, 77, and 105 may reflect a distortion in the conformation of the thioredoxin. Structural studies of human (Qin *et al.*, 1994 and Qin *et al.*, 1995) and *Anabaena* (Saarinen, 1995) thioredoxins seem to indicate that conformational changes occur in this region upon binding to and activation of target enzymes. Thus, mutation of these regions may have impaired the ability of these thioredoxins to undergo these necessary conformational changes upon binding PRK.

CHAPTER 4

EXAMINATION OF THE FEASIBILITY OF USING FLUORESCENCE ANISOTROPY AS A DIRECT MEASURE OF THE BINDING AFFINITIES OF THE THIOREDOXINS FOR THEIR TARGET ENZYMES

To this point, characterization of the Trx *f* mutants K58E, ΔN74, N74D, Q75D, ΔN77, T105I, and V89I/T105I has entailed a determination of the kinetic parameters of V_{max} and $S_{0.5}$. The $S_{0.5}$ value is typically viewed as reflective of the affinity of the target proteins for Trx. However, it is actually a complex composite of multiple rate constants and, consequently, may differ from a true dissociation constant. Thus, a direct measurement of the binding affinities of Trx *f* and mutants thereof for FBPase, MDH, and PRK is desirable. This chapter describes an attempt to establish such a method based on fluorescence polarization.

Under steady-state conditions resulting from the constant illumination of a sample, the fluorescence polarization of a molecule is proportional to the rotational relaxation time (i.e., the time it takes the molecule to rotate through a 68.5° angle). In turn, the rotational relaxation time is dependent upon viscosity (η), the effective molecular volume of the fluorescent molecule (V), absolute temperature (T), and the gas constant (R) in the following manner: rotational relaxation time = $3\eta V/RT$. Consequently, if η and T are held constant, fluorescence polarization is directly related to the molecular volume. Molecular volume changes can arise from binding or dissociation of two molecules or conformational changes. Hence, if a fluorescently tagged ligand binds to its receptor, the resulting increase in the rotational relaxation time will be represented by an increase in fluorescence polarization. (For a review of this background information, see Lakowicz, 1983.)

To detect fluorescence polarization, monochromatic light is passed through a vertical polarizing filter to excite fluorescent molecules in the sample. The molecules that are oriented properly in the plane absorb light, are excited, and consequently, emit light which is measured in both the horizontal and vertical directions. Polarization can then be calculated in the following manner:

Polarization = $(\text{intensity}_{\text{vertical}} - \text{intensity}_{\text{horizontal}}) / (\text{intensity}_{\text{vertical}} + \text{intensity}_{\text{horizontal}})$.

For completely polarized light, $\text{intensity}_{\text{horizontal}} = 0$ and polarization = 1.0 while in the case of natural or unpolarized light, $\text{intensity}_{\text{horizontal}}$ and $\text{intensity}_{\text{vertical}}$ are equivalent and the polarization is consequently zero. In essence, polarization provides a quantitative determination of the extent of molecular rotation during the period between excitation and emission. In general, small molecules rapidly rotate relative to the rapid emission of fluorescent light and, therefore, have a low polarization value. Large molecules will have high polarization values since they rotate slowly. As already mentioned, then, the fluorescence polarization of a fluorescently-tagged small protein will rise upon binding to a target. In this chapter, anisotropy, rather than polarization values, are reported due to the greater ease with which they can be mathematically manipulated. Anisotropy is mathematically related to polarization in the following manner: anisotropy = 2P / (3-P), where P is the polarization value.

The technique of fluorescence anisotropy as a tool for determining binding affinities has several advantages over other methods (Jameson and Sawyer, 1995; Lundblad *et al.*, 1996). Fluorescence anisotropy allows for a direct, nearly instantaneous measure of the ratio of bound ligand to free ligand. With this technique, a physical separation of bound ligand from that which is free is avoided. The high sensitivity of the fluorescence anisotropy technique also makes it appealing.

Isatoic anhydride, through a reaction with a hydroxyl group on ribose units, has

been used fairly extensively to generate fluorescent analogs (*o*-aminobenzoyl derivatives) of GTP, ATP, cAMP, cGMP (Hiratsuka, 1982; Hiratsuka, 1983) as well as tRNA (Servillo *et al.,* 1993). Churchich (1993) reasoned that isatoic anhydride is likely to be an ideal reagent for generating derivatized proteins that are suitable for fluorescence anisotropy studies, as the *o*-aminobenzoyl chromophore generated from reaction of this reagent with nucleophilic groups on a protein (as shown below in Reaction 1) is small and, therefore, would probably cause only minor conformational alterations.

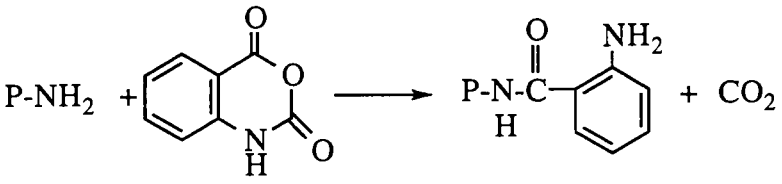

Reaction 1

In his experiments, Churchich was able to demonstrate a 1:1 stoichiometry of labeling of *E. coli* Trx (one mole of chromophore incorporated per mole of protein), with the derivatized protein having a maximal absorption at 330 nm and a maximal fluorescence emission at 435 nm (these maxima are distinct from those of an underivatized protein). The emission anisotropy of this material was 0.040. His study of protein-protein interactions entailed a titration of the oxidized form of derivatized Trx with varying concentrations of BSA. Through anisotropy measurements, a K_d of 2 μM was obtained.

EXPERIMENTAL PROCEDURES

Materials

The following materials were obtained from their indicated sources: isatoic anhydride and iodoacetic acid, Aldrich; pure recombinant *E. coli* Trx, Promega Corp.;

TPCK-treated trypsin, Worthington Biochemical Corp.; guanidine hydrochloride, DTT, Tris, Bicine, and Hepes, Research Organics; BME and EDTA, Sigma; and ammonium bicarbonate, Fisher Scientific.

Purification of Enzymes

The recombinant form of spinach Trx *f* was expressed and purified to homogeneity as in Chapter 2. Pure recombinant spinach Trx *m* was kindly provided by Professor Peter Schürmann (Université de Neuchâtel, Switzerland). The concentrations of the thioredoxin stock solutions were determined using the appropriate extinction coefficients and molecular weight values (i.e., *E. coli* Trx: 13,700 $M^{-1}cm^{-1}$, 11,700 g/mol; Trx *f*: 17,700 $M^{-1}cm^{-1}$, 13,567 g/mol; and Trx *m*: 20,500 $M^{-1}cm^{-1}$, 13,384 g/mol). Spinach FBPase was partially purified as described in Chapter 2. Spinach PRK was purified to homogeneity and oxidized as described in Chapter 3.

Activation of FBPase and PRK

Initial rates of FBPase activation were determined as in Chapter 2. Initial rates of oxidized PRK activation were determined as in Chapter 3, with the background rate due to activation by 4 mM DTT alone being subtracted from the rate in the presence of Trx to determine the Trx-dependent rate of activation.

Fluorescence Measurements

All fluorescence measurements were conducted with a SLM-Aminco-Bowman Series 2 Luminescence Spectrometer equipped with filter wheels. Bandpasses for both the excitation and emission monochromators were 4 nm. The optics for anisotropy measurements were set in an L-configuration.

RESULTS

Establishing a Procedure For Labeling Trx With Isatoic Anhydride

The following procedure was developed for the effective derivatization of *E. coli* Trx: A 200-µl labeling reaction was performed in a 500-µl eppendorf tube containing a spin vane. The reaction contained 100 mM potassium phosphate (pH 7.8), 1 mM EDTA, and 2 mg/ml Trx. A four-fold molar excess of isatoic anhydride was added every 10 minutes from a 7 mg/ml stock in methanol that was prepared fresh every 20 minutes. The reaction was allowed to proceed for one hour at room temperature with constant stirring. Glycerol (20 µl) was then added to the reaction , and the entire mixture was then applied to a Pharmacia NAP-10 column (*i.e.*, a prepacked disposable column containing Sephadex G-25 Medium of DNA grade; the column volume is 5 ml) which had just been equilibrated with 10 column volumes of 100 mM potassium phosphate (pH 7.8)/1 mM EDTA/5 mM DTT/10% glycerol. Fractions (200 µl) were collected, and the absorbance of each fraction at 280 nm and 330 nm was determined (Fig. 4-1A). The fractions containing Trx were pooled and reapplied to the NAP-10 column. The Trx was eluted with the buffer just described and 400-µl fractions were collected (Fig. 4-1B). The pooled fractions contained Trx which had been labeled with a stoichiometry of 1:1. (The degree of labeling was determined spectrophotometrically using the extinction coefficient of 4,600 $M^{-1}cm^{-1}$ at 330 nm.) This labeling procedure is a modified version of that which has been published (Churchich, 1993), as utilization of the published procedure yielded substoichiometric labeling. Also, an attempt was made to remove the excess free reagent by dialysis rather than gel filtration by employing double-sided spin biodialysers (Sialomed, Inc.) with membranes having a molecular weight cut-off of 2000. However, dialysis of the reaction mixtures for two days at 4°C failed to remove all of the excess reagent.

The procedure which proved to consistently produce stoichiometrically labeled (1:1)

wild-type Trx *f* involved the following: The reaction was as described in the preceding paragraph except 2 mM DTT was present and the isatoic anhydride stock solution was 5 mg/ml. Removal of the excess reagent was also as described above except the elution buffer contained 100 mM potassium phosphate (pH 7.8)/1 mM EDTA/5 mM DTT/15% glycerol. The derivatized Trx *f* (*i.e.*, *o*-aminobenzoyl Trx *f*) used in all the studies described below was obtained through this procedure. A control reaction was performed in which wild-type Trx *f* was subjected to the complete procedure just described except isatoic anhydride was excluded from the labeling reaction. This Trx *f* is referred to as "control Trx" in the remainder of this chapter and corresponding figures.

Spinach Trx *m* was subjected to the labeling procedure used for Trx *f*, except the reaction was allowed to proceed for only 45 minutes since the mixture began to appear cloudy after that point. Following elution from the NAP-10 column with 100 mM potassium phosphate (pH 7.8)/1 mM EDTA/5 mM DTT/15% glycerol, the Trx was pooled and dialyzed overnight against 100 mM potassium phosphate (pH 7.8)/1 mM EDTA/5 mM DTT/20% glycerol. The stoichiometry was only 1:2 (label:Trx) following these manipulations and, consequently, the Trx was subjected to a second labeling reaction. This second reaction (in a 200-µl volume) contained Trx at a concentration of 1 mg/ml, 3.5 mM DTT, 100 mM potassium phosphate (pH 7.8), and 1 mM EDTA. The mixture was stirred at room temperature for 20 minutes, with an equimolar amount of isatoic anhydride being added every 10 minutes. The reaction was applied to a NAP-10 column and eluted with 100 mM potassium phosphate (pH 7.8)/1 mM EDTA/5 mM DTT/15% glycerol. Those fractions containing Trx were pooled and the stoichiometry of labeling was determined to be 0.6:1 (label:Trx).

Properties of Derivatized Trx

Derivatized Trx *f* (labeled with a stoichiometry of 1:1), upon excitation at 330 nm,

displays an emission maxima at 435 nm (Fig. 4-2). Control Trx *f*, as anticipated, shows negligible fluorescence emission upon excitation at 330 nm. Upon excitation at 280 nm, the control Trx *f* shows an emission spectra typical of proteins, with a single peak appearing which has a maximum value at approximately 345 nm (Fig. 4-3). Surprisingly, two fluorescence emission peaks appear upon excitation of derivatized Trx *f* at 280 nm. The first peak coincides with that found in the control sample, while the second peak has a maximum at 445 nm. A similar phenomenon was observed with *o*-aminobenzoyl *E.coli* Trx, with excitation at 330 nm displaying a maximal emission at approximately 420 nm and excitation at 280 nm giving emission maxima at 345 and 410 nm. The average steady state emission anisotropy value for derivatized Trx *f* alone is 0.1254. Derivatized Trx *m* possesses a similar anisotropy value of 0.1388.

The stability of the fluorescent tag-Trx linkage was examined by two approaches. In one case, the pH of a derivatized Trx *f* solution was adjusted to 13 with KOH and allowed to stand at room temperature for one hour. The Trx was then applied to a Pharmacia NAP-10 column and eluted with a buffer composed of 100 mM potassium phosphate/1mM EDTA/5 mM DTT/10% glycerol. No apparent loss of fluorescent tag occurred with this treatment. In the second case, excess isatoic anhydride was removed from labeling reactions with *E. coli* Trx and Trx *f* through gel filtration (NAP-10 column). In each case, the fractions containing labeled thioredoxin were pooled, guanidine was added to a final concentration of 4.5 M, and the samples were left at room temperature for one hour. The samples were then applied to NAP-10 columns which had been equilibrated with buffer containing 4.5 M guanidine. Examination of the material eluted from the gel filtration column indicated that no apparent loss of the fluorescent tag from the proteins occurred. In addition to demonstrating the stability of the fluorescent tag-Trx linkage, this second approach also verifies the effectiveness with which gel filtration removes fluorescent reagent which is noncovalently bound to the Trx.

Does Derivatization of Trx *f* Impact the Kinetics of Target Enzyme Activation?

To assess whether the presence of the fluorescent tag on the Trx impacts the apparent affinity ($S_{0.5}$ value) of the Trx for its target enzymes or thioredoxin's ability to activate its targets, initial rates of activation of FBPase and PRK were determined with *o*-aminobenzoyl-wild-type Trx *f* (labeled with a stoichiometry of 1:1). The rates of activation were compared to those obtained with control Trx *f*. As shown in figure 4-4, the labeled Trx is capable of activating FBPase, displaying a V_{max} (75 mU/min) that is similar to that of a control sample of Trx (62 mU/min). The apparent affinity of the derivatized Trx for FBPase, however, is greatly reduced; while the $S_{0.5}$ value with the control Trx is 2.3 μM, it is 23 μM with the derivatized protein.

The impact of the derivatization on the ability of Trx to activate PRK was even more dramatic than that observed with FBPase. While derivatized Trx, at concentrations of up to 20 μM, is able to activate PRK, higher concentrations actually inhibit the normal background activation by DTT alone (compare figure 3-2A with 4-5A). This observation is not unique to the derivatized Trx, as the Trx subjected to a "control" labeling reaction displays the same characteristics. To determine if the presence of methanol during the labeling reaction (which is normally introduced with the isatoic anhydride) is the source of the deleterious effect on Trx, a sample of wild-type Trx *f* was treated with 5.5% methanol (*i.e.*, the highest concentration of MeOH that Trx is ever exposed to during the labeling reaction) for one hour at room temperature without stirring. Following removal of the methanol from the sample by means of a NAP-10 column, the Trx was shown to be capable of activating PRK in a normal fashion, displaying a V_{max} of 6 mU/min and a $S_{0.5}$ of 20 μM (values nearly identical to those in Table 3-1) (Fig. 4-5B). Therefore, mechanical forces present during the labeling procedure (e.g., constant stirring of the

reaction mixture), but not methanol, are apparently causing the surface of the Trx to become partially denatured.

Determination of Binding Affinities of Derivatized Wild-Type Chloroplastic Thioredoxins for PRK by Fluorescence Anisotropy

The binding of *o*-aminobenzoyl derivatives of wild-type Trx *f* and Trx *m* to PRK was directly examined through fluorescence anisotropy studies using an excitation wavelength of 330 nm and an emission wavelength of 435 nm (Fig. 4-6). From the increases in anisotropy observed during the addition of increasing concentrations of PRK to the thioredoxins, K_d values were calculated. (Note that in a control experiment, addition of buffer alone did not cause an alteration in anisotropy values.) Despite the fact that derivatized Trx *f* is seriously impaired in its ability to activate PRK, it is still capable of binding to this target, as demonstrated by a K_d of 35.2 μM +/- 5.3 μM. The K_d for derivatized Trx *m* and PRK was determined to be 69.1 μM +/- 24.9 μM. For comparison purposes, recall from Chapter 3 that the $S_{0.5}$ values were 17 μM and 15 μM for Trx *f* and Trx *m*, respectively.

Attempts to Identify Site of Incorporation of Fluorescent Label

The approach employed for the identification of the site(s) of modification of Trx involved complete tryptic digestion, peptide purification, and sequencing of fluorescent peptide(s) by automated Edman degradation. Identification of the amino acid to which the fluorescent tag was covalently bound would then involve searching for a blocked residue in the sequence. For complete digestion of Trx with trypsin, it was necessary to first *S*-carboxymethylate the protein. *o*-Aminobenzoyl Trx *f* was treated with IAA (15 mM) in a solution containing 4.5 M guanidine, 50 mM Tris-HCl (pH 8.3), 3 mM EDTA, and 5 mM

DTT for 1.5 hours at room temperature in the dark. The reaction was then quenched by adding BME to a final concentration of 30 mM and dialyzed against 60 mM NH_4HCO_3/1 mM BME for 3-4 hours and then overnight against 60 mM NH_4HCO_3. For digestion, the *S*-carboxymethylated protein was treated with trypsin (1%) for 5 hours at 37°C, a second addition of trypsin (1%) was then made, and incubation continued overnight. Analyses of aliquots of the digests by SDS-PAGE on Pharmacia high density PhastGels indicated that complete digestion indeed occurred.

The tryptic digest was diluted with HPLC-grade water to give an ammonium bicarbonate concentration of 12 mM and was then injected onto a TosoHaas TSK gel DEAE 5PW column (3.3 ml) equilibrated with 12 mM NH_4HCO_3. Peptide elution was monitored by absorbance at 215 nm with a LDC SpectroMonitor 4100 programmable variable wavelength detector and by fluorescence with a Perkin Elmer 650 fluorescence detector with the excitation wavelength set at 330 nm and the emission wavelength set at 435 nm. Following injection, the column was washed with 12 mM NH_4HCO_3 until the absorbance at 215 nm and the fluorescence returned to baseline. A series of four gradients (all with a flow rate of 1 ml/min) was then run: Gradient #1 was from 12-60 mM NH_4HCO_3 in 24 min., gradient #2 was from 160-200 mM NH_4HCO_3 in 70 min., gradient #3 was from 200-100 mM NH_4HCO_3 in 15 min., and gradient #4 was from 100 mM NH_4HCO_3 to 100 mM NH_4HCO_3 /1M NaCl in 66 min. Only one fluorescent peak appeared during this chromatographic procedure. This peak, which coincided with a peptide peak, eluted isochratically in 12 mM NH_4HCO_3 prior to the initiation of gradient #1. Fractions corresponding to this peak were pooled and subjected to sequencing. Although the peak routinely appeared to be symmetrical, two peptide sequences were

evident. The predominant peptide had the sequence LLEAIQAA, consistent with the first Leu being residue 112 (Fig. 4-7). The second peptide had the sequence VTEVNK, making the first Val residue 17. Surprisingly, sequencing did not reveal evidence for a blocked residue. Intact (*i.e.,* undigested) *o*-aminobenzoyl Trx *f* was subsequently subjected to sequencing. Qualitatively the sequencing yielded results identical to those of unlabeled Trx (*i.e.,* approximately the first 50 residues of Trx can be sequenced without difficulty in both cases). It was then suspected that the fluorescent tag was being hydrolyzed from the Trx during the *S*-carboxymethylation or tryptic digestion. To test this hypothesis, the elution pattern of hydrolyzed isatoic anhydride in the preceding chromatographic procedure needed to be determined. Hydrolyzed isatoic anhydride was generated by increasing the pH of a solution of isatoic anhydride in 100 mM potassium phosphate/1 mM EDTA to 12 with KOH and allowing the solution to stand at room temperature overnight. This hydrolyzed reagent was then chromatographed using the procedure just described and was found to elute isochratically in 60 mM NH_4HCO_3 (shortly after gradient #1). A tryptic digested sample of *o*-aminobenzoyl Trx *f* which had been spiked with hydrolyzed isatoic anhydride was also chromatographed in the same manner. Two fluorescent peaks appeared in this case, one eluting isochratically in 12 mM NH_4HCO_3 and the other eluting isochratically in 60 mM NH_4HCO_3. Thus, the fluorescent tag-Trx bond is apparently not being cleaved prior to sequencing. Several modified versions of this chromatographic procedure were also tried with the tryptic digested, *o*-aminobenzoyl Trx *f* and tryptic digested, *o*-aminobenzoyl *E.coli* Trx and all attempts to sequence peptides corresponding to fluorescent peaks failed to identify a blocked residue. Therefore, elucidation of the site of modification has not been possible.

DISCUSSION

A procedure was developed in which the chloroplastic thioredoxins Trx *f* and Trx *m*, as well as *E.coli* Trx, were covalently modified with the fluorescent reagent isatoic anhydride. The derivatized chloroplastic thioredoxins have similar steady-state emission anisotropy values as expected for proteins of similar size. An interesting characteristic of the derivatized thioredoxins is the occurrence of fluorescence resonance energy transfer from the tryptophan residues (2 of which exist in spinach Trx *f* and *E.coli* Trx) to the chromophore upon excitation at 280 nm, as noted by the appearance of a second peak in the emission spectra at 445 nm. Thus, the fluorescent tag and the tryptophans of Trx are apparently in close proximity (10-100 Å). Upon excitation at 330 nm, the derivatized, but not the underivatized, material displays a fluorescence peak in the region of 435 nm. This phenomenon made the monitoring of the *o*-aminobenzoyl protein conjugates in the presence of other proteins possible.

The binding affinity (K_d) of *o*-aminobenzoyl Trx *f* for PRK was determined to be approximately 35 μM by emission anisotropy. This value is twice that of the $S_{0.5}$ value obtained by kinetic analyses in Chapter 3 and much greater than that obtained through "kinetic" studies by Gontero *et al.* (1993) (0.8 μM). The K_d value for PRK and *o*-aminobenzoyl Trx *m* was determined to be 69 μM, although the standard deviation associated with this value (25 μM) is larger than in the Trx *f* study. The $S_{0.5}$ value obtained by kinetic analyses with Trx *m* and PRK was 4.5 times smaller (Table 3-1). Thus, as was concluded in Chapter 3, the affinities of the chloroplastic thioredoxins for PRK are not dramatically different. In addition, the $S_{0.5}$ values reported in Chapter 3 can probably be regarded as fairly good measurements of the ability of the thioredoxins to bind PRK.

Given the small size of the *o*-aminobenzoyl moiety, the observation that the

derivatization of Trx *f* greatly impairs its ability to activate FBPase is surprising. This result may be due to the apparent damage that Trx has accrued during the labeling reaction. Alternatively, the fluorescent tag may be covalently attached to a residue important for Trx-FBPase interaction. As the derivatized Trx is somehow negatively altered in its ability to activate PRK, presumably due to partial surface denaturation of the Trx during the labeling procedure, the K_d value determined by anisotropy may not be a measure of the true K_d.

Since the site of modification of Trx may be important for binding to targets, identifying this site is desirable. Unfortunately, all attempts to do so have failed. The linkage between the fluorescent tag and Trx may be unstable during Edman degradation, consequently precluding the appearance of a "blocked" residue in the sequence. Modification of the glutamate residues in each of the two tryptic peptides highlighted in Fig. 4-7 could yield such a result since ester linkages are inherently unstable. Lysyl residues were mentioned by Churchich (1993) as being likely candidates for modification. The expected amide linkage, however, should be stable.

Prior to extended use of the technique described herein for the direct determination of the K_d values for Trx and its target enzymes, modifications in the protocol are needed. Trx needs to be derivatized without simultaneously being damaged. This may simply involve the elimination of the stirring during the labeling reaction. If successful labeling of Trx proves to be impossible under milder reaction conditions, additional fluorescent reagents can employed. An alternative to fluorescence for studying binding is microcalorimetry. This technique does require greater quantities of protein, however, than anisotropy.

REFERENCES

REFERENCES

Aguilar, F., Brunner, B., Gardet-Salvi, L., Stutz, E., and Schürmann, P. (1992) *Plant Mol. Biol.* **20,** 301-306

Aragnol, D., Pradel, J., and Cecchini, J.-P. (1985) *Biochim. Biophys. Acta* **829,** 275-281

Avron, M. and Gibbs, M. (1974) *Plant Physiol.* **53,** 136-139

Besse, I. and Buchanan, B. (1997) *Bot. Bull. Acad. Sin.* **38,** 1-11

Brandes, H. K., Stringer, C. D., and Hartman, F. C. (1992) *Biochemistry* **31,** 12833-12838

Brandes, H. K., Larimer, F. W., Geck, M. K., Stringer, C. D., Schürmann, P., and Hartman, F. C. (1993) *J. Biol. Chem.* **268,** 18411-18414

Brandes, H. K., Larimer, F. W., and Hartman, F. C. (1996a) *J. Biol. Chem.* **271,** 3333-3335

Brandes, H. K., Hartman, F. C., Lu, T.-Y., and Larimer, F. W. (1996b) *J. Biol. Chem.* **271,** 6490-6496

Buchanan, B. B. (1980) *Ann. Rev. Plant Physiol. Plant Mol. Biol.* **31,** 341-374

Buchanan, B. B. (1984) *BioScience* **34,** 378-383

Buchanan, B. B. (1986) *Thioredoxin and Glutaredoxin Systems: Structure and Function* (Holmgren, A., Bränden, C.-I., Jörnvall, H., and Sjöberg, B.-M., eds) pp. 233-242, Raven Press, New York

Buchanan, B. B. (1991) *Arch. Biochem. Biophys.* **288,** 1-9

Buchanan, B. B. (1992) *Trends in Photosynthesis Research* (Barber, J., Guerrero, M. G., and Medrano, H., eds.) 171-183, Intercept Ltd. Andover, U.K.

Buchanan, B. B., Schürmann, P., and Jacquot, J.-P. (1994a) *Seminars in Cell Biology* **5,** 285-293

Buchanan, B. B., Schürmann, P., Decottignies, P., and Lozano, R. M. (1994b) *Arch. Biochem. Biophys.* **314,** 257-260

Champigny, M.-L. and Bismuth, E. (1976) *Physiol. Plant.* **36,** 95-100

Charles, S. and Halliwell, B. (1980) *Biochem. J.* **185,** 689-693

Chen, Y. and Xu, G.-J. (1996) *Biochem. Mol. Biol. Intern.* **39,** 941-948

Chivers, P., Laboissière, M., and Raines, R. (1996) *EMBO J.* **15,** 2659-2667

Chivers, P., Prehoda, K., and Raines, R. (1997) *Biochemistry* **36,** 4061-4066

Churchich, J. E. (1993) *Analytical Biochem.* **213,** 229-233

Clancey, C. J. and Gilbert, H. F. (1987) *J. Biol. Chem.* **262,** 13545-13549

Clasper, S., Chelvarajan, R., Easterby, J. S., and Powls, R. (1994) *Biochim. Biophys. Acta* **1209,** 101-106

Crawford, N. A., Yee, B. C., Hutcheson, S. W., Wolosiuk, R. A., and Buchanan, B. B. (1986) *Arch. Biochem. Biophys.* **244,** 1-15

Creighton, T. E. and Freedman, R. B. (1993) *Curr. Biol.* **3,** 790-793

de Lamotte-Guery, F., Miginiac-Maslow, M., Decottignies, P., Stein, M., Minard, P., and Jacquot, J.-P. (1991) *Eur. J. Biochem.* **196,** 287-294

Decottignies, P., Schmitter, J.-M., Miginiac-Maslow, M., Marechal, P., Jacquot, J.-P., and Gadal, P. (1988) *J. Biol. Chem.* **263,** 11780-11785

Dyson, H. J., Gippert, G. P., Case, D. A., Holmgren, A., and Wright, P. E. (1990) *Biochemistry* **29,** 4129-4136

Dyson, H. J., Jeng, M.-F., Tennant, L., Slaby, I., Lindell, M., Cui, D.-S., Kuprin, S., and Holmgren, A. (1997) *Biochemistry* **36,** 2622-2636

Edman, J.C., Ellis, L., Blacher, R.W., Roth, R., and Rutter W. (1985) *Nature* **317,** 267-270

Eklund, H., Gleason, F., and Holmgren, A. (1991) *Proteins: Structure, Function, and Genetics* **11,** 13-28

Fickenscher, K. and Scheibe, R. (1988) *Arch. Biochem. Biophys.* **260,** 771-779

Fischer, K. and Latzko, E. (1979) *Biochem. Biophys. Res. Comm.* **89,** 300-306

Freedman, R., Hirst, T., and Tuite, M. (1994) *Trends Biochem. Sci.* **19,** 331-336

Geck, M. K., Larimer, F. W., and Hartman, F. C. (1996) *J. Biol. Chem.* **271,** 24736-24740

Gietl, C. (1992) *Biochem. Biophys. Acta* **1100,** 217-234

Gilbert, H. F. (1995) *Methods Enzymol.* **251,** 8-28

Gilbert, H. F., McLean, V., and McLean, M. (1990) *Adv. Enzymol.* **63,** 69-172

Gleason, F. K. (1992) *J. Bacteriol.* **174,** 2592-2598

Gontero, B., Cárdenas, M., and Ricard, J. (1988) *Eur. J. Biochem.* **173,** 437-443

Häberlein, I. and Vogeler, B. (1995) *Biochim. Biophys. Acta* **1253,** 169-174

Hatch, M. and Agostino, A. (1992) *Plant Physiol.* **100,** 360-366

Hermoso, R., Castillo, M., Chueca, A., Lazaro, J., Sahrawy, M., and Lopez-Gorge, J. (1996) *Plant Mol. Biol.* **30,** 455-465

Hiratsuka, T. (1982) *J. Biol. Chem.* **257,** 13354-13358

Hiratsuka, T. (1983) *Biochem. Biophys. Acta* **742,** 496-508

Hodges, M., Miginiac-Maslow, M., Decottignies, P., Jacquot, J.-P., Stein, M., Lepiniec, L., Cretin, C., and Gadal, P. (1994) *Plant Mol. Biol.* **26,** 225-234

Holmgren, A. (1985) *Ann. Rev. Biochem.* **54,** 237-271

Holmgren, A. (1989) *J.Biol. Chem.* **264,** 13963-13966

Hosur, M., Sainis, J., and Kannan, K. (1993) *J. Mol. Biol.* **234,** 1274-1278

Issakidis, E., Miginiac-Maslow, M., Decottignies, P., Jacquot, J.-P., Cretin, C., and Gadal, P. (1992) *J. Biol. Chem.* **267,** 21577-21583

Issakidis, E., Decottignies, P., and Miginiac-Maslow, M. (1993) *FEBS Letters* **321,** 55-58

Issakidis, E., Saarinen, M., Decottignies, P., Jacquot, J.-P., Cretin, C., Gadal, P., and Miginiac-Maslow, M., (1994) *J.Biol. Chem.* **269,** 3511-3517

Issakidis, E., Lemaire, M., Decottignies, P., Jacquot, J.-P., and Miginiac-Maslow, M. (1996) *FEBS Letters* **392,** 121-124

Jackson, R., Sessions, R., and Holbrook, J. (1992) *J. Comp. Aided Mol. Des.* **6,** 1-18

Jacquot, J-P., Lopez-Jaramillo, J., Chueca, A., Cherfils, J., Lemaire, S., Chedozeau, B., Miginiac-Maslow, M., Decottignies, P., Wolosiuk, R., and Lopez-Gorge, J. (1995) *Eur. J. Biochem.* **229,** 675-681

Jacquot, J-P., Lopez-Jaramillo, J., Miginiac-Maslow, M., Lemaire, S., Cherfils, J., Chueca, A., and Lopez-Gorge, J. (1997) *FEBS Letters* **401,** 143-147

Jameson, D. and Sawyer, W. (1995) *Methods Enzymol.* **246,** 283-300

Jeng, M.-F., Campbell, A. P., Begley, T., Holmgren, A., Case, D.A., Wright, P. E., and Dyson, H. J. (1994) *Structure* **2,** 853-868

Katti, S. K., LeMaster, D. M., and Eklund, H. (1990) *J. Mol. Biol.* **212,** 167-184

Kraulis, P. J. (1991) *J. Appl. Cryst.* **24,** 946-950

Kunkel, T. A., Roberts, J. D., Zakour, R. A. (1987) *Methods Enzymol.* **154,** 367-382

Laing, W. A., Stitt, M., and Heldt, H.W. (1981) *Biochem. Biophys. Acta* **637,** 348-359

Lakowicz, J. R. (1983) *Principles of Fluorescence Spectroscopy* Plenum Press, New York

Latzko, E., Garnier, R., and Gibbs, M. (1970) *Biochem. Biophys. Res. Comm.* **39,** 1140-1144

Law, M., Charles, S., and Halliwell, B. (1983) *Biochem. J.* **210,** 899-903

Leatherbarrow, R. J. (1987) *Enzfitter: A Non-linear Regression Data Analysis Program for the IBM PC/PS2* Biosoft, Ferguson, MO

Leegood, R. and Walker, D. (1980) *Biochem. Biophys. Acta* **593,** 362-370

Li, D., Stevens, F., Schiffer, M., and Anderson, L. (1994) *Biophysical J.* **67,** 29-35

Lim, C.-J., Sa, J.-H., Fuchs, J. (1996) *Biochem. Biophys. Acta* **1307,** 13-16

Loferer, H. and Hennecke, H. (1994) *Trends Biochem. Sci.* **19,** 167-171

Lundblad, J., Laurence, M., and Goodman, R. (1996) *Molecular Endocrinology* **10,** 607-612

Marcus, F., Harrsch, P.B., Moberly, L., Edelstein, I., and Latshaw, P.S. (1987) *Biochem.* **26,** 7029-7035

Marcus, F., Moberly, L., and Latshaw, S. (1988) *Proc. Nat. Acad. Sci.* **85,** 5379-5383

Marcus, F. and Harrsch, P. (1990) *Arch. Bioch. Biopys.* **279,** 151-157

Marcus, F., Chamberlain, S., Chu, C., Masiarz, F., Shin, S., Yee, B., and Buchanan, B. (1991) *Arch. Biochem. Biophys.***287,** 195-198

Martin, J. (1995) *Structure* **3,** 245-250

McKinney, D., Buchanan, B., and Wolosiuk, R. (1979) *Biochem. Biophys. Res. Comm.* **86,** 1178-1184

Milanez, S., Mural, R.J., and Hartman, F.C. (1991) *J. Biol. Chem.* **266,** 10694-10699

Mittard, V., Blackledge, M., Stein, M., Jacquot, J.-P., Marion, D., and Lancelin, J.-M. (1997) *Eur. J. Biochem.* **243,** 374-383

Nishizawa, A. N. and Buchanan, B. B. (1981) *J. Biol. Chem.* **256,** 6119-6126

Ochertina, O., Harnecker, J., Rother, T., Schmid, R., and Scheibe, R. (1993) *Biochem. Biophys. Acta* **1163,** 10-16

Ochertina, O. and Scheibe, R. (1994) *FEBS Letters* **355,** 254-258

Porter, M. A. and Hartman, F. C. (1986) *Biochemistry* **25,** 7314-7318

Porter, M. A., Milanez, S., Stringer, C. D., and Hartman, F. C. (1986) *Arch. Bioch. Biopys.* **245,** 14-23

Porter, M. A., Stringer, C., and Hartman, F. C. (1988) *J. Biol. Chem.* **263,** 123-129

Porter, M. A. and Hartman, F. C. (1988) *J. Biol. Chem.* **263,** 14846-14849

Porter, M. A., Potter, M. D., and Hartman, F. C. (1990) *J. Protein Chem.* **9,** 445-451

Pradel, J., Soulie, J.-M., Buc, J., Meunier, J.-C., and Ricard, J. (1981) *Eur. J. Biochem.* **113,** 507-511

Qin, J., Clore, G. M., and Gronenborn, A. M. (1994) *Structure* **2,** 503-522

Qin, J., Clore, G. M., Poindexter Kennedy W. M., Huth, J. R., and Gronenborn, A. M. (1995) *Structure* **3,** 289-297

Rault, M., Gontero, B., and Ricard, J. (1991) *Eur. J. Biochem.* **197,** 791-797

Rault, M., Giudici-Orticoni, M.-T., Gontero, B., and Ricard, J. (1993) *Eur. J. Biochem.***217,** 1065-1073

Reng, W., Riessland, R., Scheibe, R., and Jaenicke, R. (1993) *Eur. J. Biochem.* **217,** 189-197

Rivera-Madrid, R., Mestres, D., Marinho, P., Jacquot, J.-P., Decottignies, P., Miginiac-Maslow, M., and Meyer, Y. (1995) *Proc. Nat. Acad. Sci.* **92,** 5620-5624

Rodriguez-Suarez, R. J., Mora-García, S., and Wolosiuk, R. (1997) *Biochem. Biophys. Res. Comm.* **232,** 388-393

Romanova, A. and Pavlovets, V. (1997) *Russ. J. Plant Physiol.* **44,** 230-238

Saarinen, M., Gleason, F. K., and Eklund, H. (1995) *Structure* **3,** 1097-1108

Sainis, J. K. and Harris, G. C. (1986) *Biochem. Biophys. Res. Comm.* **139,** 947-954

Sainis, J. K., Merriam, K., and Harris, G. C. (1989) *Plant Physiol.* **89,** 368-374

Salamon, Z., Tollin, G., Hirasawa, M., Gardet-Salvi, L., Stritt-Etter, A.-L., Knaff, D. B., and Schürmann, P. (1995) *Biochim. Biophys. Acta* **1230,** 114-118

Sambrook, J., Fritsch, E. F., and Maniatis, T. (1989) *Molecular Cloning: A Laboratory Manual*, 2nd Ed., Cold Spring Harbor Laboratory, Cold Spring Harbor, NY

Sanger, F., Nicklen, S., and Coulson, A.R. (1977) *Proc. Natl. Acad. Sci. U.S.A.* **74,** 5463-5467

Scheibe, R. (1981) *FEBS Letters* **133,** 301-304

Scheibe, R., Fickensher, K., and Ashton, A. R. (1986) *Biochim. Biophys. Acta* **870,** 191-197

Scheibe, R. (1990) *Bot. Acta* **103,** 327-334

Scheibe, R., Kampfenkel, K., Wessels, R., and Tripier, D. (1991) *Biochim. Biophys. Acta* **1076,** 1-8

Schürmann, P., Maeda, K., and Tsugita, A. (1981) *Eur. J. Biochem.* **116,** 37-45

Servillo, L., Balestrier, C., Quagliuolo, L., Iorio, E., and Giovane, A. (1993) *Eur. J. Biochem.* **213,** 583-589

Soulie, J.-M., Buc, J., Riviere, M., and Ricard, J. (1985) *Eur. J. Biochem.* **152,** 565-568

Spyrou, G., Enmark, E., Miranda-Vizuete, A., and Gustafson, J.-Å. (1997) *J. Biol. Chem.* **272,** 2936-2941

Süss, K.-H., Arkona, C., Manteuffel, R., and Adler, K. (1993) *Proc. Natl. Acad. Sci. USA* **90,** 5514-5518

Tsugita, A., Maeda, K., and Schürmann, P. (1983) *Biochem. Biophys. Res. Comm.* **115,** 1-7

Villeret, V., Huang, S., Zhang, Y., Xue, Y., and Lipscomb, W. (1995) *Biochem.* **34,** 4299-4306

Wedel, N., Clausmeyer, S., Herrmann, R. G., Gardet-Salvi, L., and Schürmann, P. (1992) *Plant Mol. Biol.* **18,** 527-533

Weichsel, A., Gasdaska, J., Powis, G., and Montfort, W. (1996) *Structure* **4,** 735-751

Wells, W., Yang, Y., and Diets, T. (1993) *Adv. Enzymol.* **66,** 149-201

Wetterauer, B., Jacquot, J.-P., and Veron, M. (1992) *J. Biol. Chem.* **267,** 9895-9904

Wolosiuk, R. A. and Buchanan, B. B. (1978) *Arch. Biochem. Biophys.* **189,** 97-101

Wolosiuk, R. A., Crawford, N. A., Yee, B. C., Buchanan, B. B. (1979) *J. Biol. Chem.* **254,** 1627-1632

Wolosiuk, R. A., Corley, E., Crawford, N., and Buchanan, B. B. (1985) *FEBS Letters* **189,** 212-216

Xia, T.-H., Bushweller, J. H., Sodano, P., Billeter, M., Björnberg, O., Holmgren, A., and Wüthrich, K. (1992) *Protein Sci.* **1,** 310-321

Zimmerman, G., Kelly, G. J., and Latzko, E. (1976) *Eur. J. Biochem.* **70,** 361-367

APPENDIX

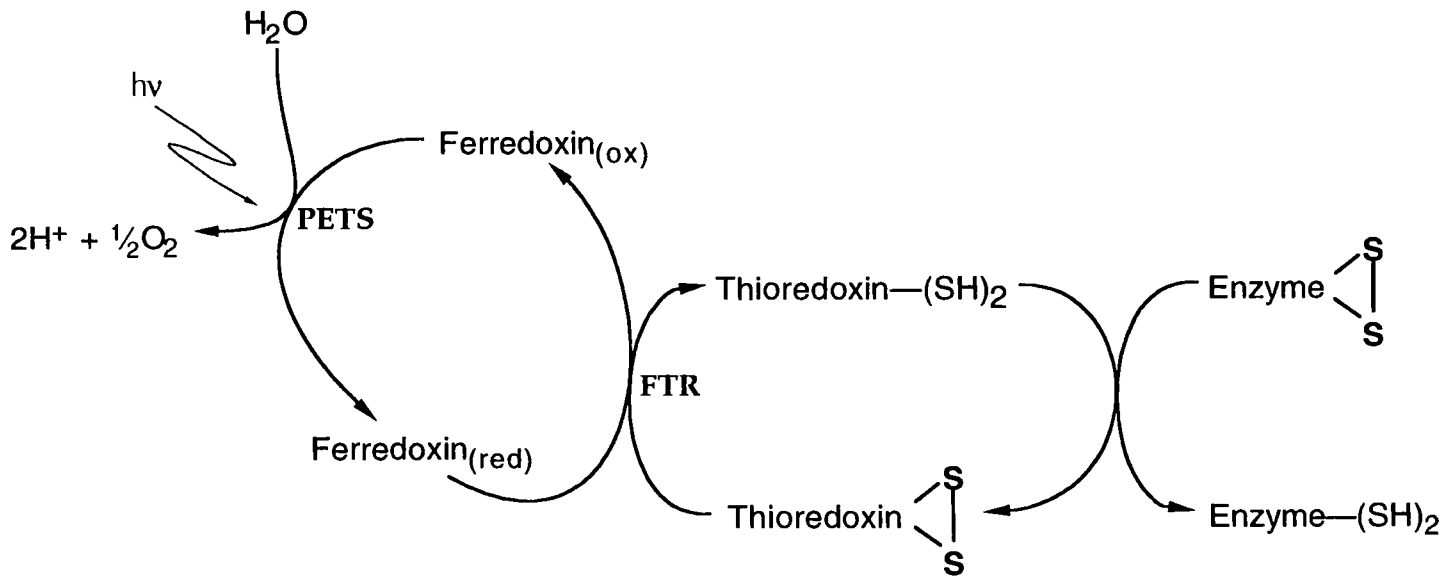

Figure 1-1: The ferredoxin/thioredoxin system as a general mechanism of light-mediated enzyme regulation. PETS denotes the photosynthetic electron transport system.

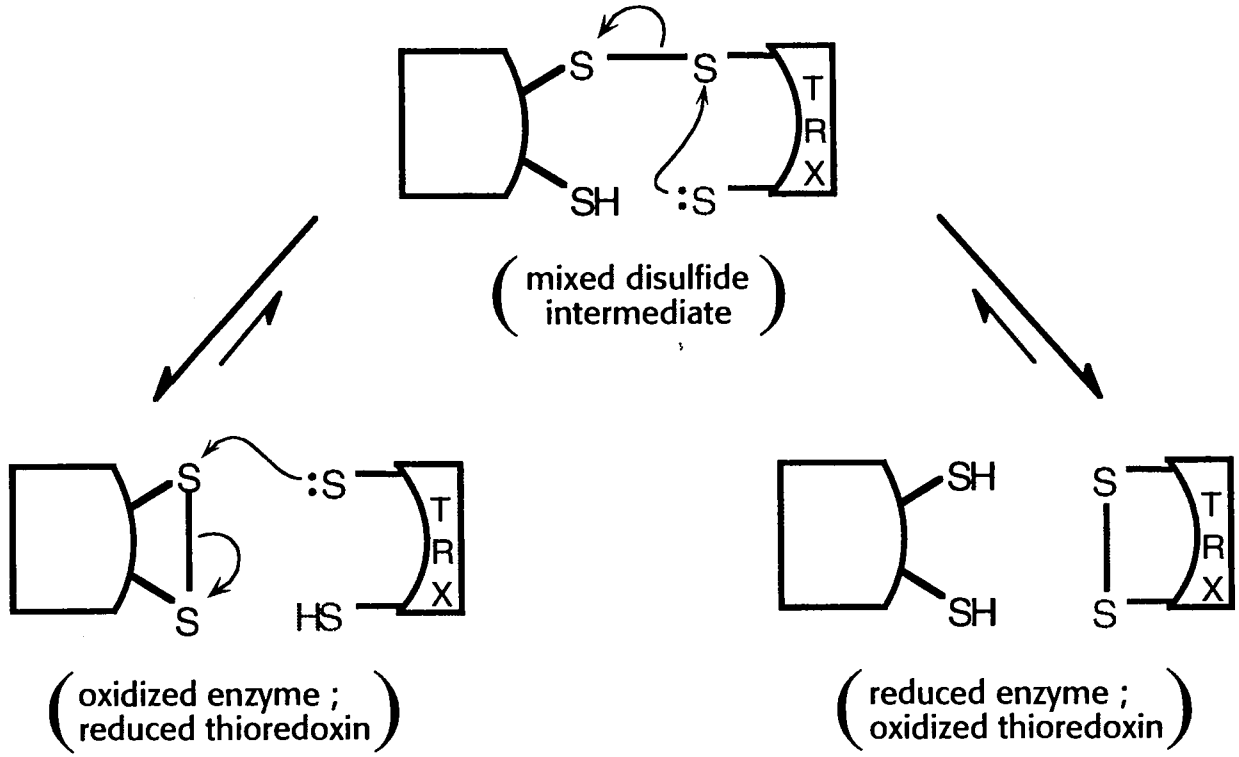

Figure 1-2: The pathway of thiol-disulfide exchange of thioredoxin.

Table 2-1. Oligonucleotides Used to Generate Site-Directed Mutants of Trx *f**

Site-Directed Mutation	Mutagenic Primer Sequence
K58E	pAAATACGAA**G**<u>A</u>**G**CTAGCAGAG
ΔN74	pGCTCGATTGT↓CAGGAAAACA
N74D	pCTCGATTGT**G**<u>A</u>**C**CAGGAAAAC
Q75D	pGATTGTAAC**G**<u>A</u>**T**GAAAACAAG
ΔN77	pCGATTGTAACCAGGAA↓AAGACATTAGCAAAGG
V89I	pGGCATCAGAGTA<u>A</u>**TT**CCTACTTTCAAGATT
T105I	pGTGGGAGAAGTTA<u>T</u>**A**GGGGCAAAATATGAT

*The bases in *bold* encode for the sites of mutation. The newly substituted bases are *underlined*. An *arrow* indicates the site of a codon deletion.

Table 2-2. Activation of FBPase by Thioredoxins at 25°C

Thioredoxin	$S_{0.5}$ (μM)	V_{max} (mU FBPase/min)	$V_{max}/S_{0.5}$ (mU FBPase/min/μM)
wild-type Trx *f*	0.9±0.2	48±2	53.3
wild-type Trx *m*	31.4±1.3	2±0.2	0.1
Trx *f*-K58E	1.5±0.1	16±1	10.7
Trx *f*-ΔN74	2.1±0.2	58±6	27.6
Trx *f*-N74D	6.3±0.4	37±2	5.9
Trx *f*-Q75D	4.0±0.3	22±1	5.5
Trx *f*-ΔN77	12.8±0.3	67±3	5.2
Trx *f*-T105I	2.0±0.1	30±1	15.0
Trx *f*-V89I/T105I	42.0±1.7	112±5	2.7

Table 2-3. Activation of MDH by Thioredoxins at 4°C

Thioredoxin	Rate constant ($M^{-1}min^{-1}$)
wild-type Trx *f*	$1.2x10^4$
wild-type Trx *m*	$9.8x10^3$
Trx *f*-K58E	$3.8x10^4$
Trx *f*-ΔN74	$3.7x10^4$
Trx *f*-N74D	$1.5x10^4$
Trx *f*-Q75D	$2.8x10^4$
Trx *f*-ΔN77	$2.4x10^4$

A.

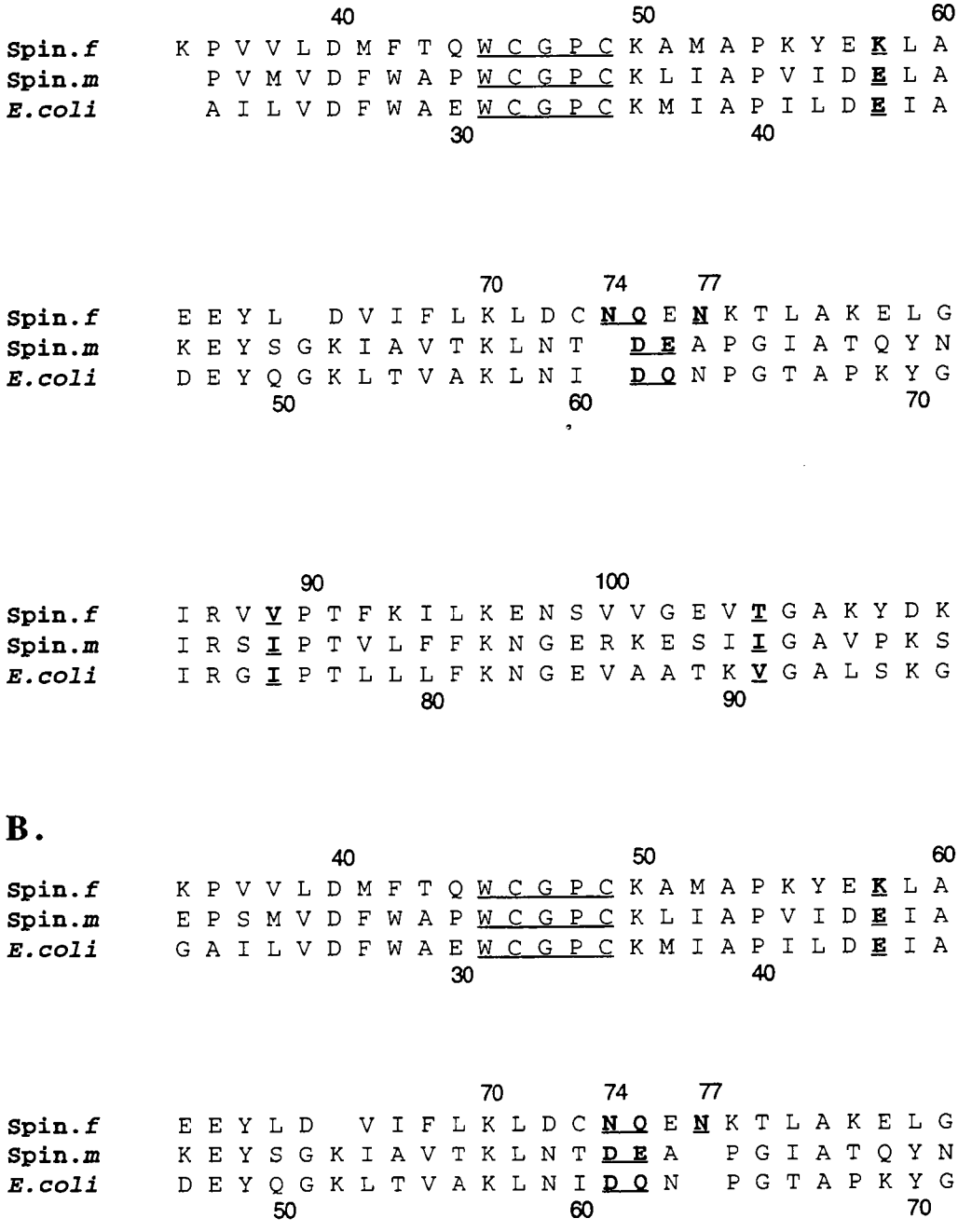

B.

Figure 2-1. Alternate sequence alignments of thioredoxins. The conserved redox active-site sequence is *underlined.* Sites of mutation are *bold* and *underlined.* Spin. *f* refers to the amino acid sequence of Trx *f* from spinach and Spin. *m* indicates the spinach Trx *m* sequence.

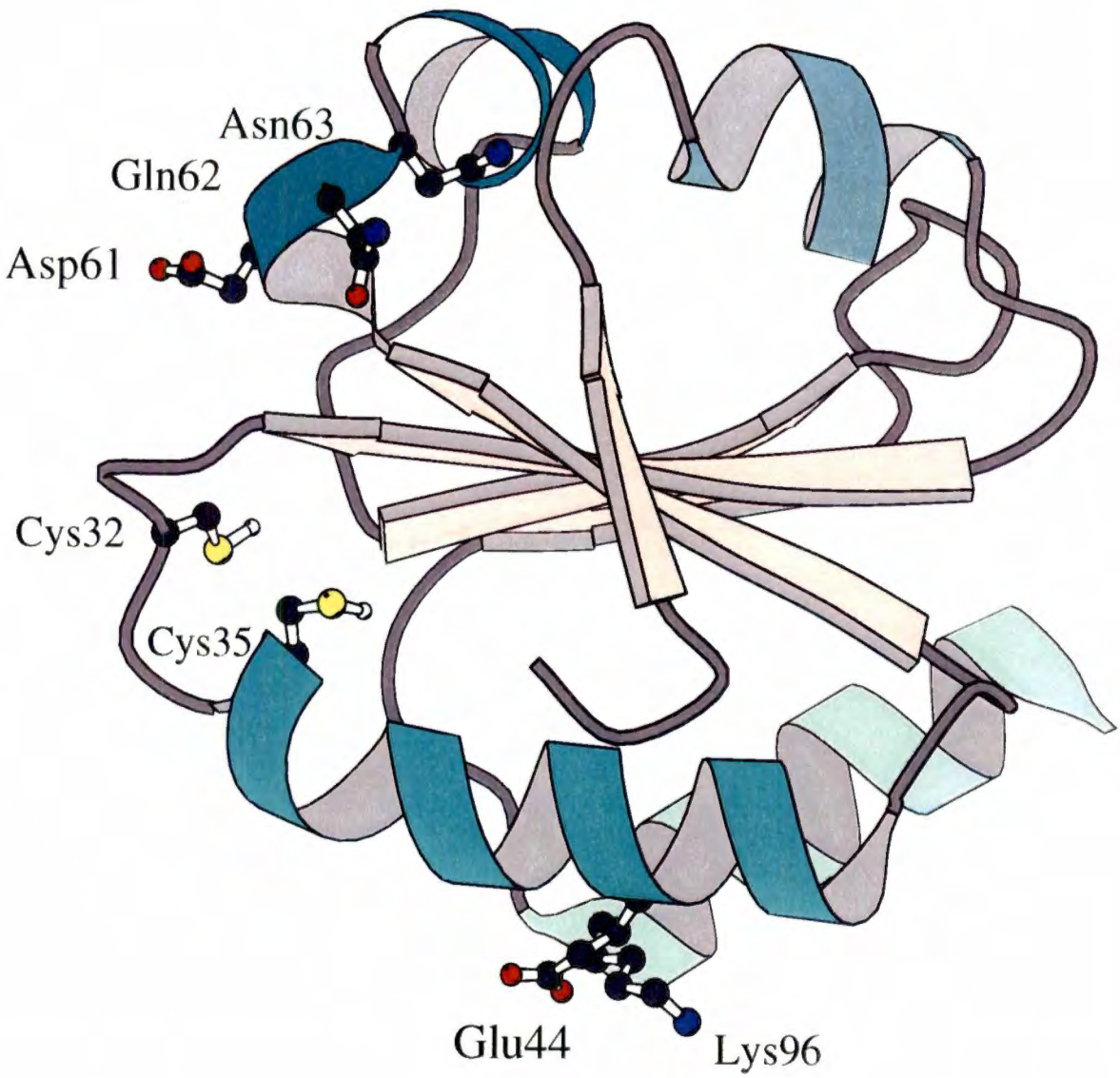

Figure 2-2: A NMR structure of reduced *E. coli* Trx. Derived from data of Dyson *et al.* (1990) and generated using MOLSCRIPT (Kraulis, 1991). Sites of mutation in Trx *f* (except for those in the putative hydrophobic contact site), the redox active cysteines, and the putative salt bridge partner of Lys58 (i.e., Glu44 in *E. coli*) are all indicated.

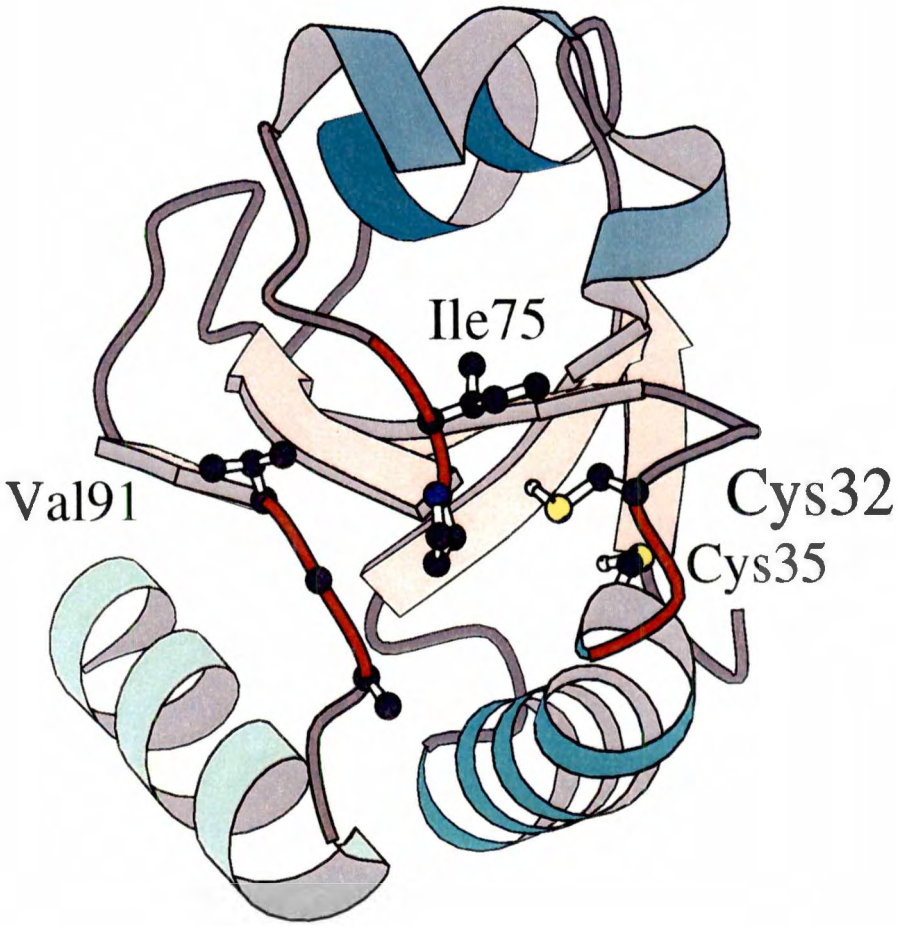

Figure 2-3: The putative hydrophobic contact site of Trx. The structure depicted in Fig. 2-2 has been rotated to yield the structure shown above. Residues forming the hydrophobic contact site are located in the red regions of three loops. Two members of the contact site, Gly33 and Pro34, are located between the indicated redox active cysteines. The two sites of mutation, Ile75 (Val89 in spinach Trx *f*) and Val91 (Thr105 in spinach *f*) are represented in ball-and-stick form, as are Pro76, Gly92, and Ala93.

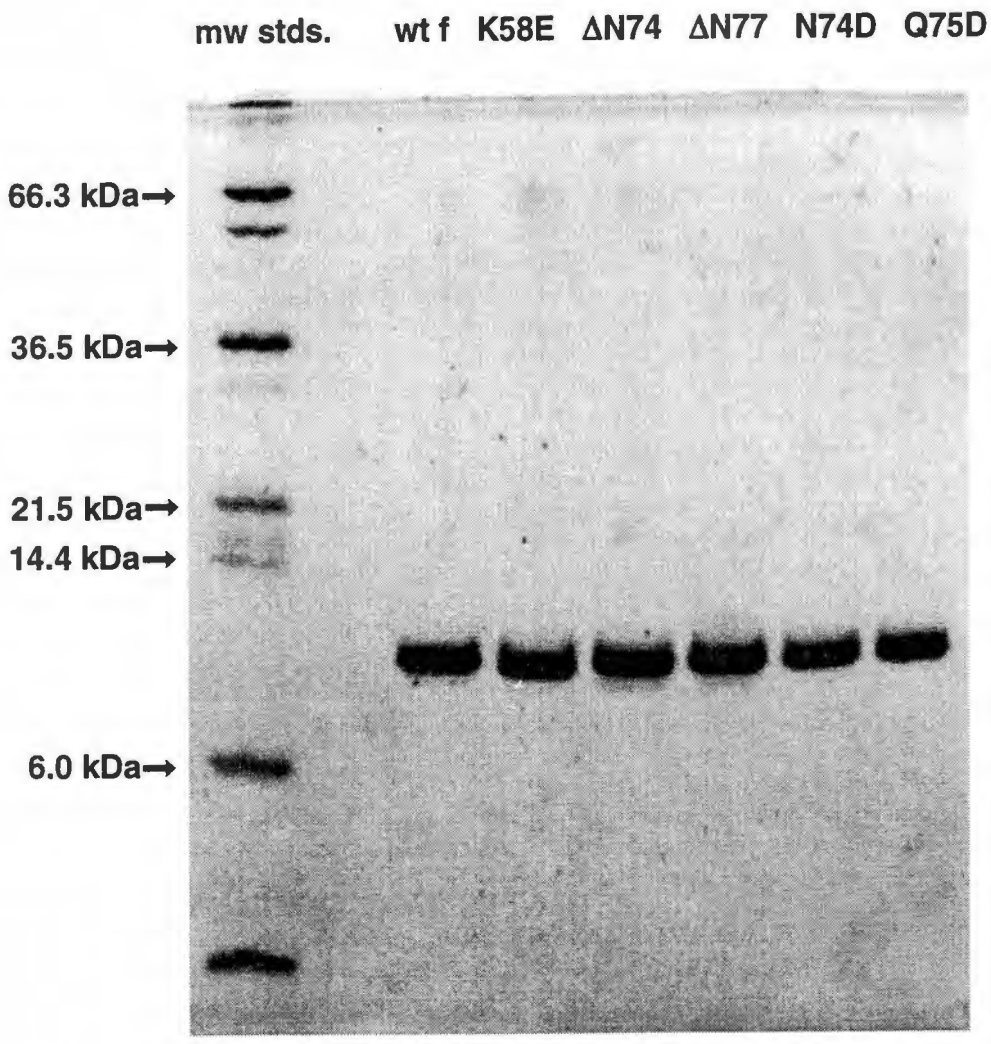

Fig. 2-4: Silver-stained SDS-PAGE of purified thioredoxins. Lane 1, Novex Mark 12 molecular weight markers; remaining lanes, 20 ng of indicated thioredoxins. The Pharmacia high density gel was digitized with the LaCie Silverscanner II at 256 dots per inch.

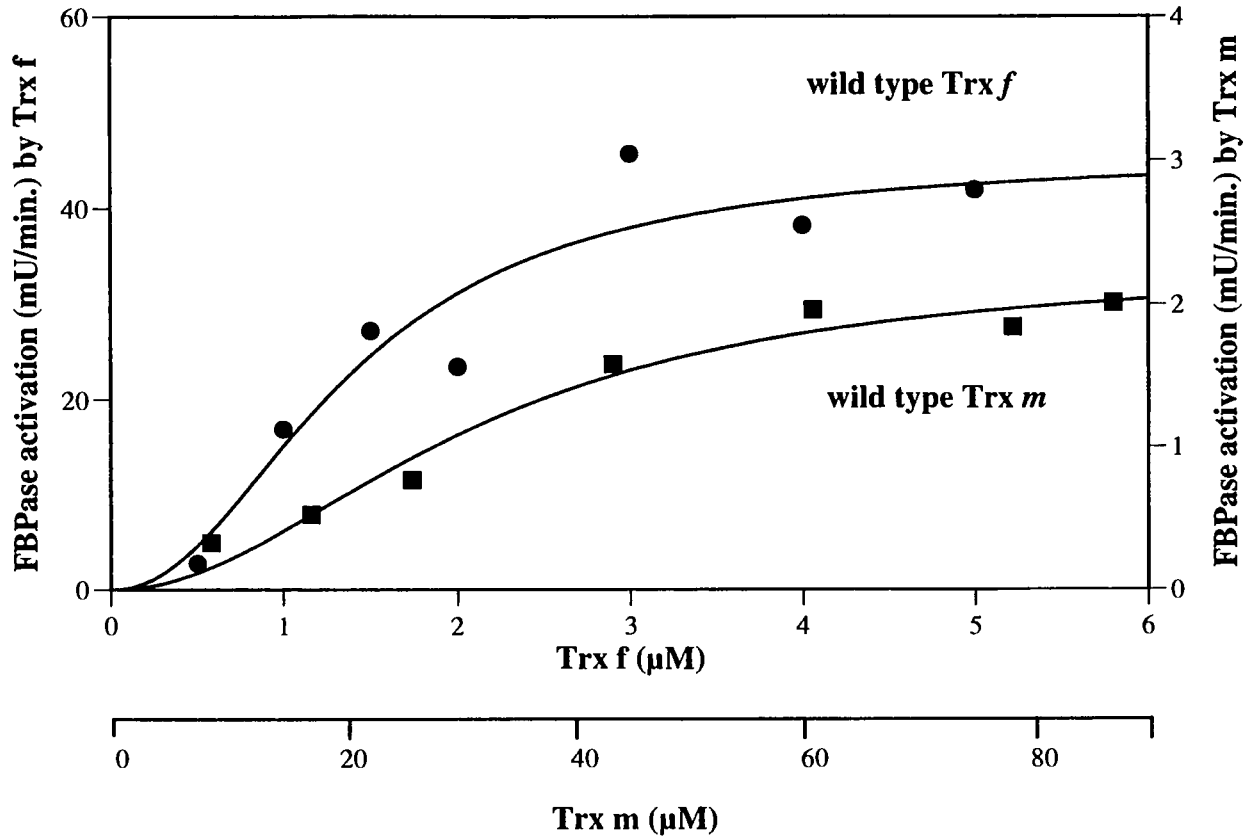

Figure 2-5: Activation of FBPase by wild-type thioredoxins. Initial rates of activation by specified concentrations and types of thioredoxins are represented by individual data points. All activations occurred at 25°C. All data were fit to the simplified Hill equation of $v = V_{max}[S]^n/(K' + [S]^n)$, where n is a calculated value for the apparent number of binding sites.

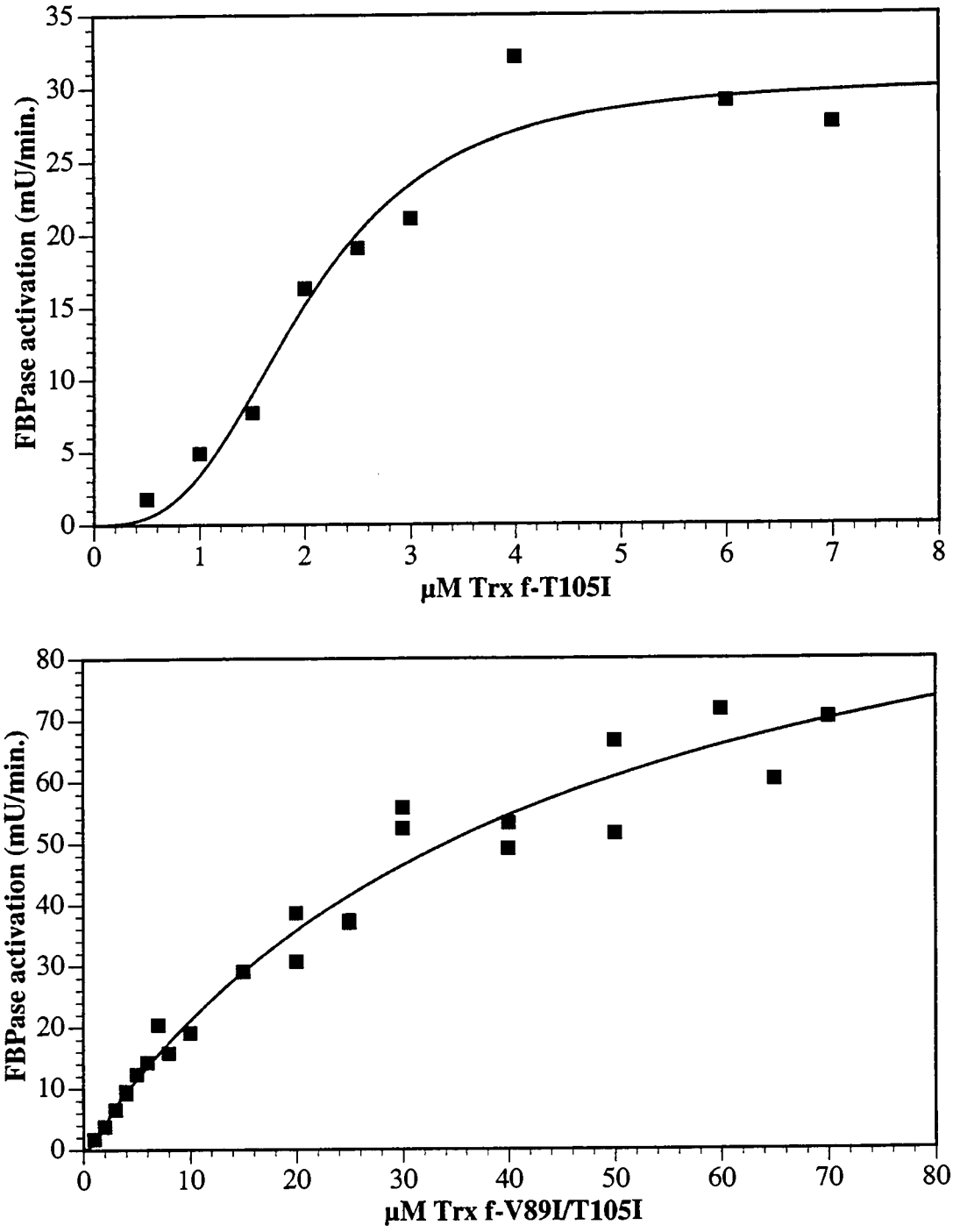

Figure 2-6: Activation of FBPase by mutant thioredoxins. Initial rates of activation by the specified concentrations and types of thioredoxins (Trx *f*-T105I, top panel; Trx *f*-V89I/T105I, bottom panel) are represented by individual data points. Curve fittings were as in Fig. 2-5.

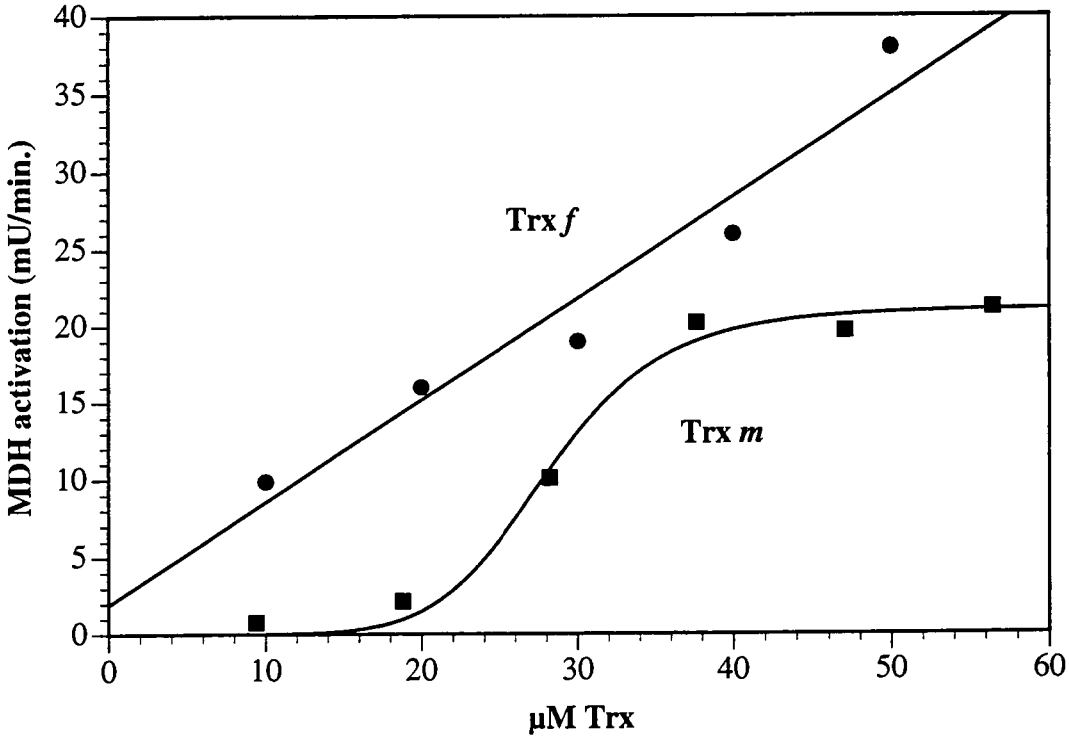

Figure 2-7: Activation of MDH by wild-type thioredoxins. Each data point indicates the initial rate of activation of MDH by the specified concentration of Trx at 4 °C. Data for Trx *m* were fit to the simplified Hill equation of $v = V_{max}[S]^n/(K' + [S]^n)$, where *n* is a calculated value for the apparent number of binding sites. Data for Trx *f* were fit to a straight line.

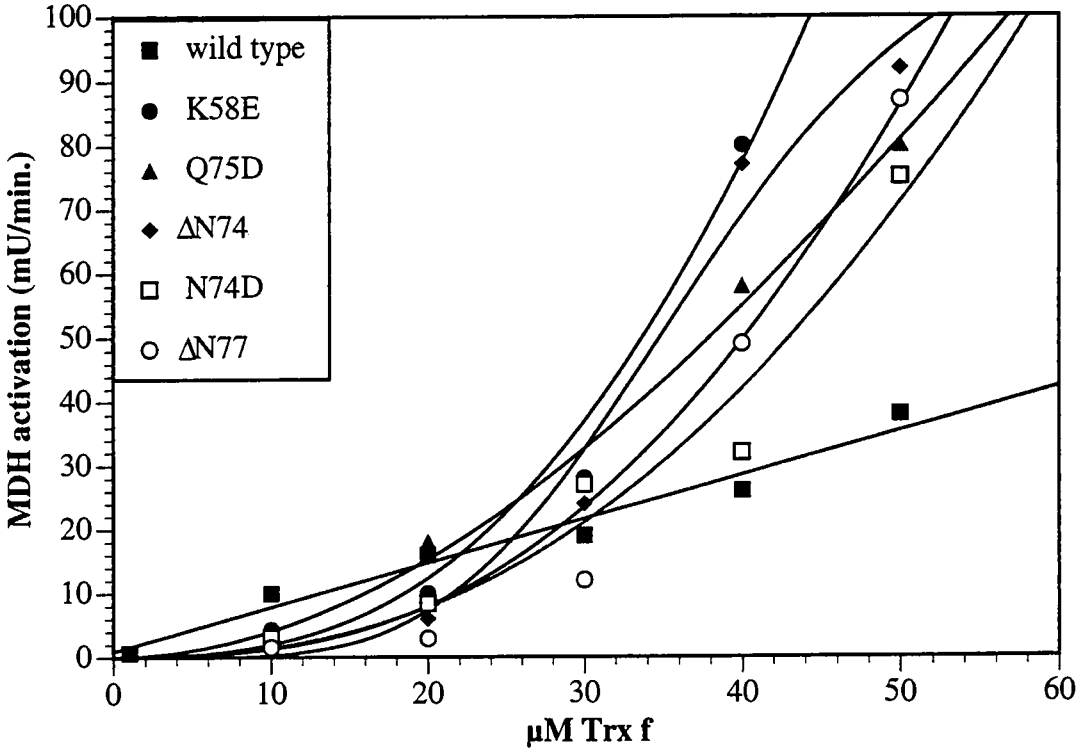

Figure 2-8: Activation of MDH by mutant thioredoxins. As in figure 2-5, each data point indicates the initial rate of activation of MDH by the specified concentration of Trx at 4 °C. Curve fittings were performed as described in figure 2-5.

Table 3-1. Activation of PRK by Thioredoxins at 25°C

Thioredoxin	$S_{0.5}$ (μM)	V_{max} (mU PRK/min)	$V_{max}/S_{0.5}$ (mU/min/μM)x100
wild-type Trx *f*	17	7	39
wild-type Trx *m*	15	11	76
Trx *f*-K58E	23	4	19
Trx *f*-ΔN74	52	20	38
Trx *f*-N74D	32	10	32
Trx *f*-Q75D	92	15	16
Trx *f*-ΔN77	47	18	38
Trx *f*-T105I	66	42	64

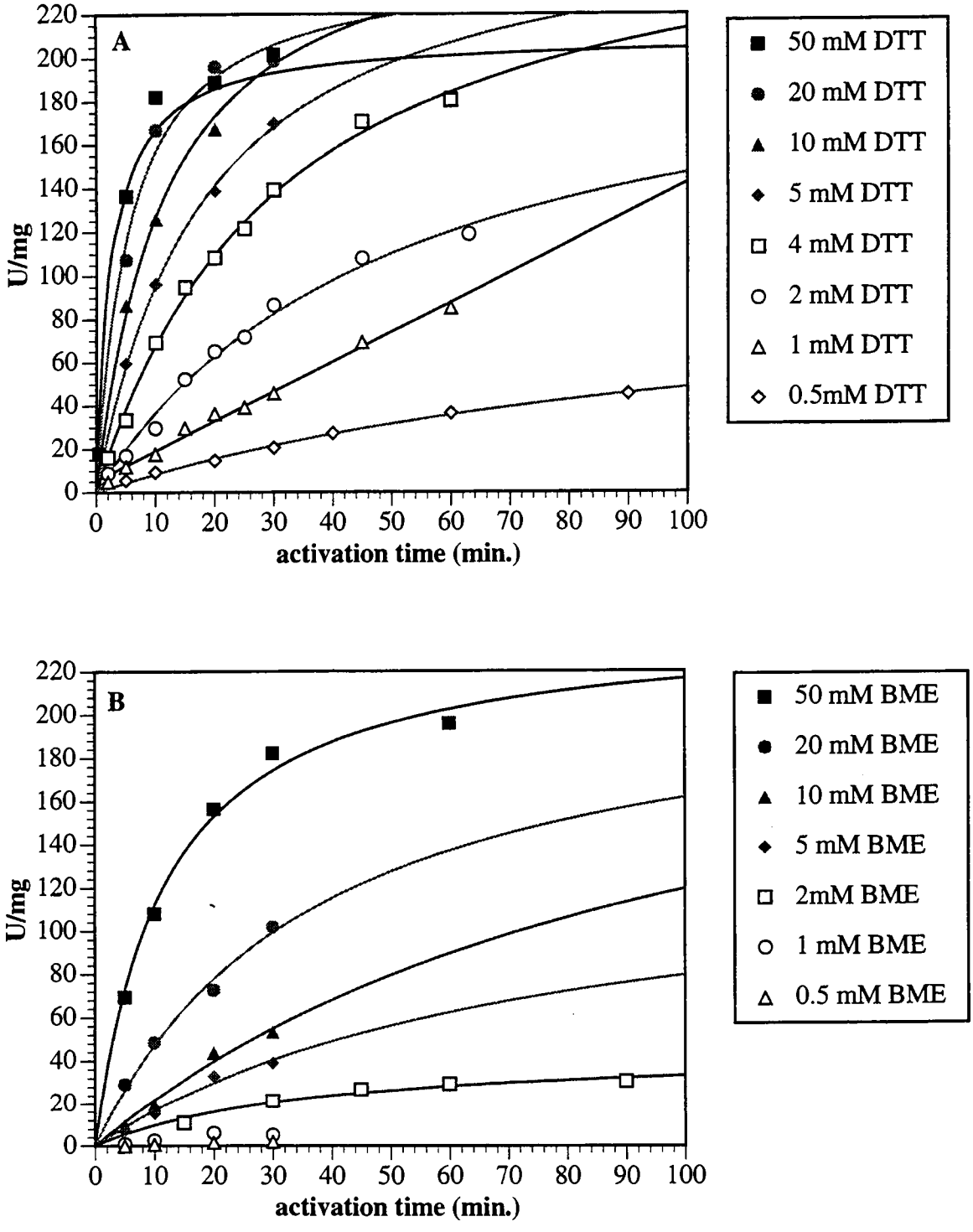

Figure 3-1: Activation of oxidized PRK by various reductants. (continued on next page)

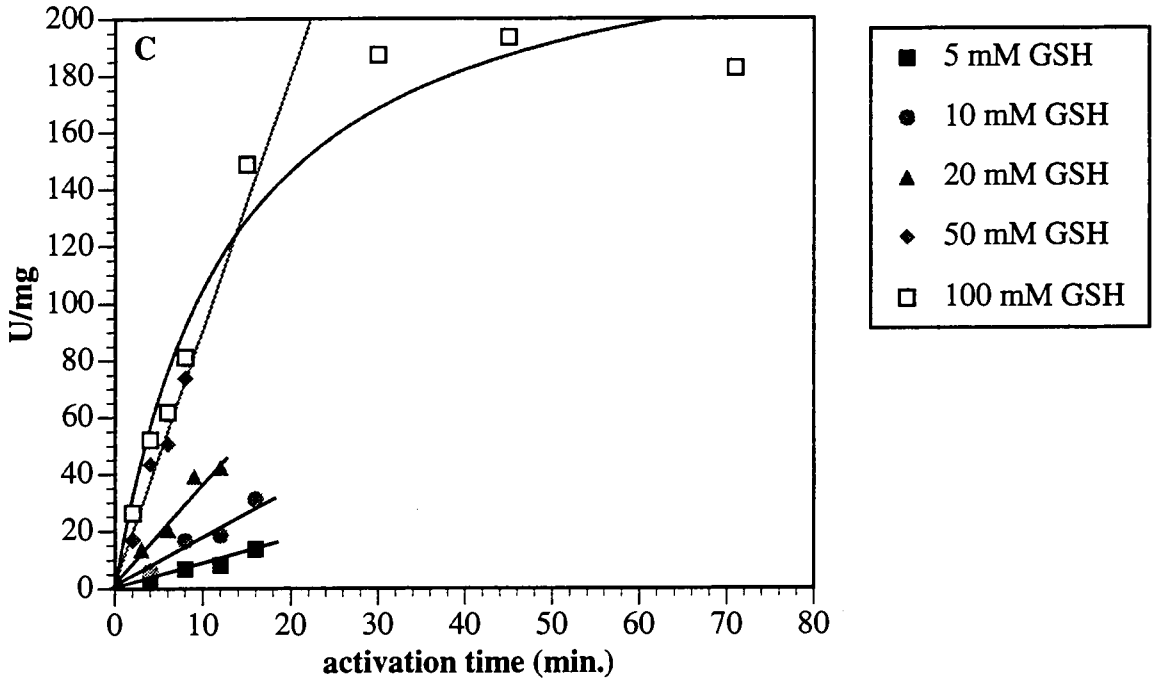

Fig. 3-1: (continued) Activation of oxidized PRK by various reductants.

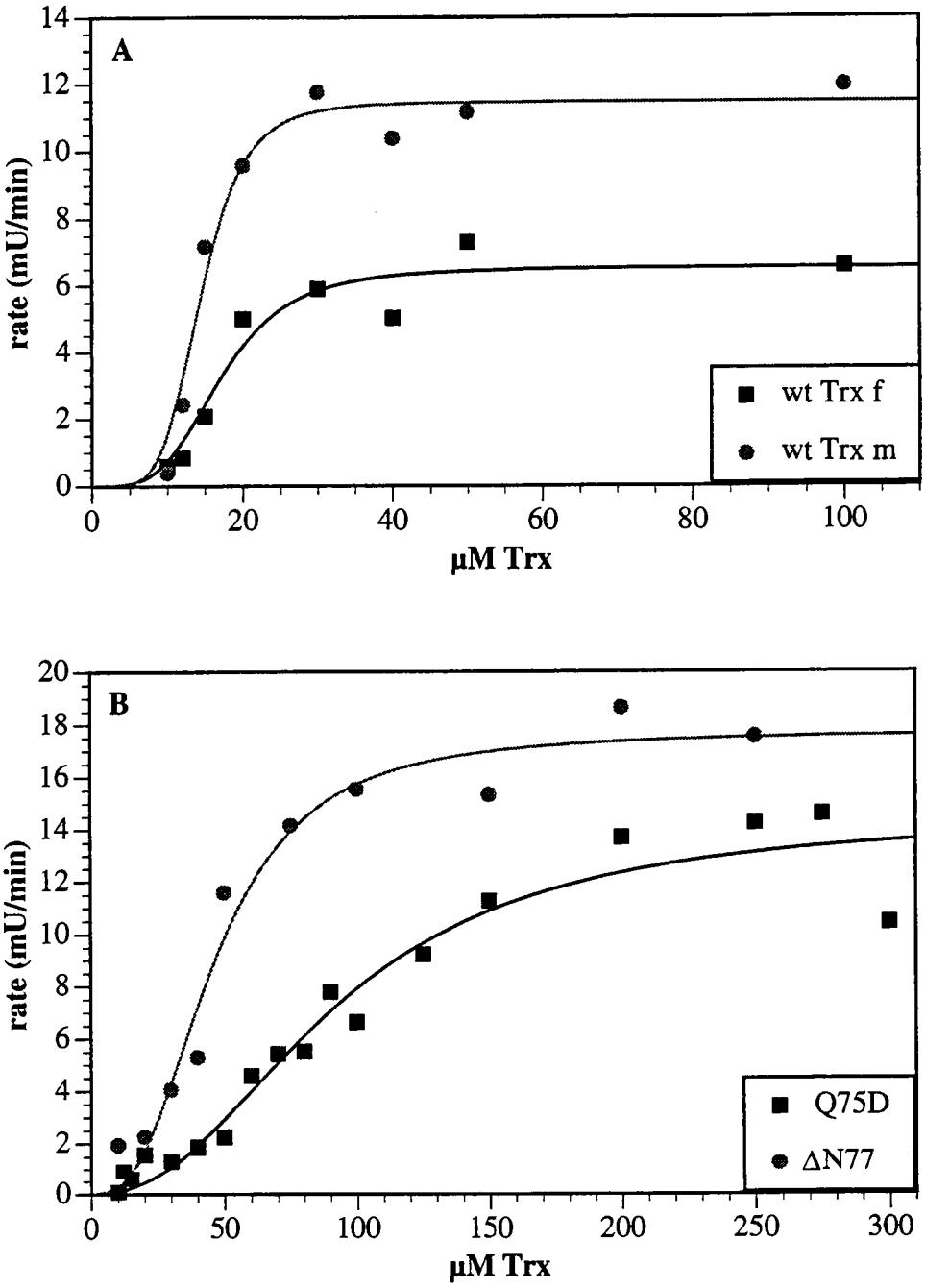

Figure 3-2: Activation of oxidized PRK by wild-type and mutant thioredoxins. Thioredoxin-dependent initial rates of activation are shown. (continued on next page)

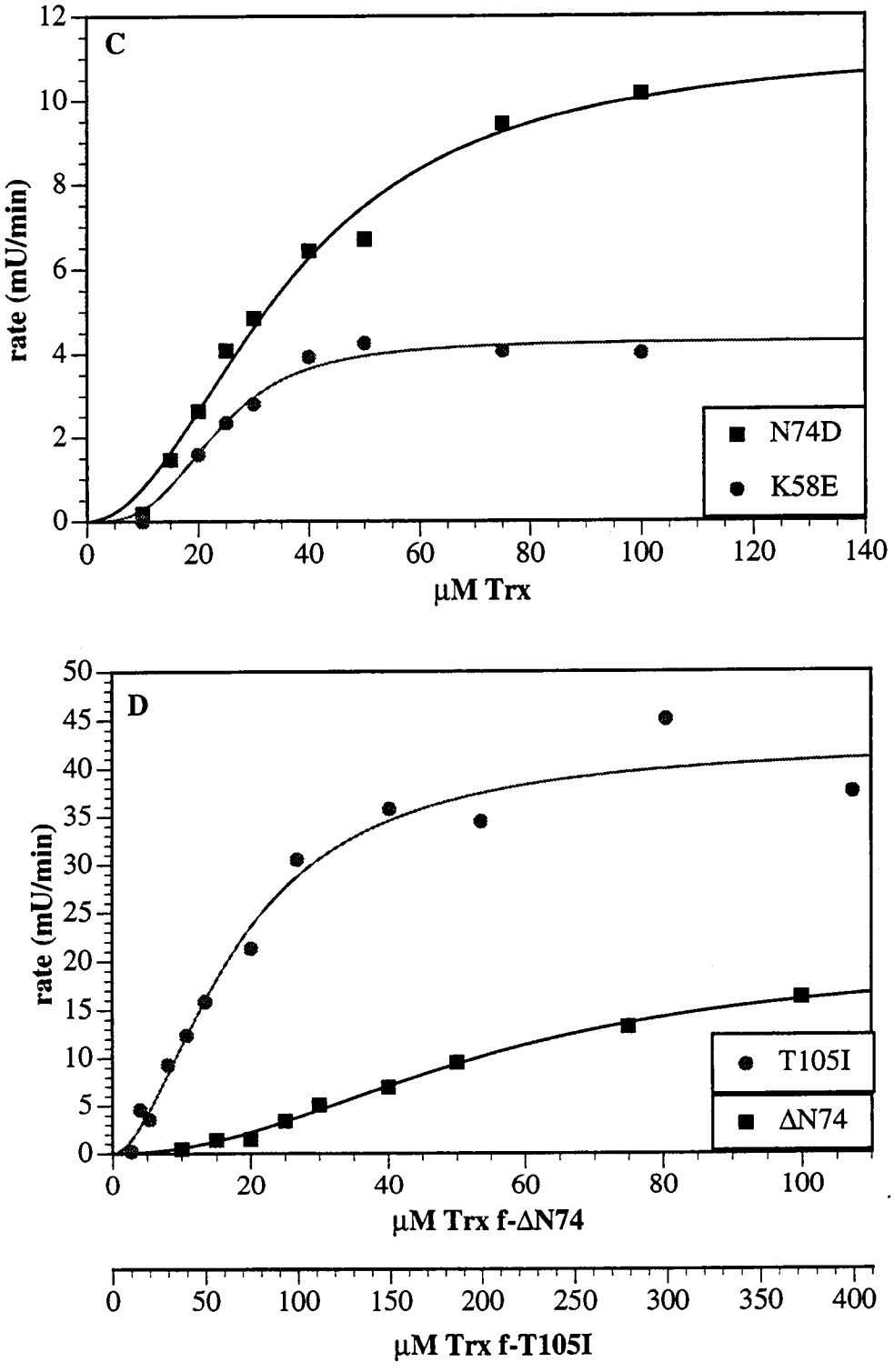

Figure 3-2: (continued) Activation of oxidized PRK by wild-type and mutant thioredoxins. Thioredoxin-dependent initial rates of activation are shown.

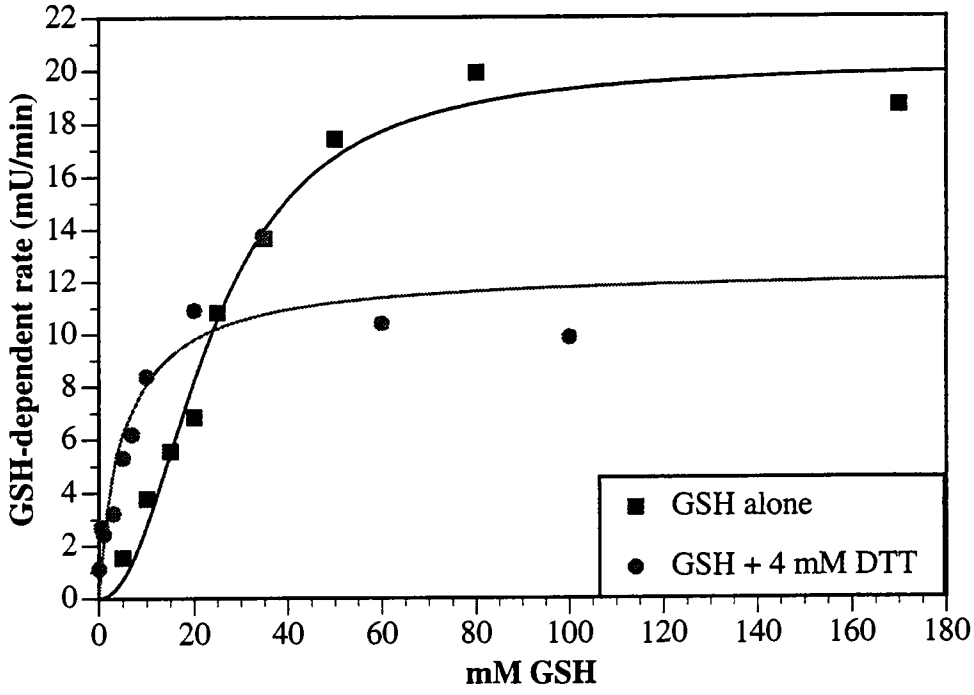

Figure 3-3: Activation of oxidized PRK by GSH in the absence and presence of 4 mM DTT

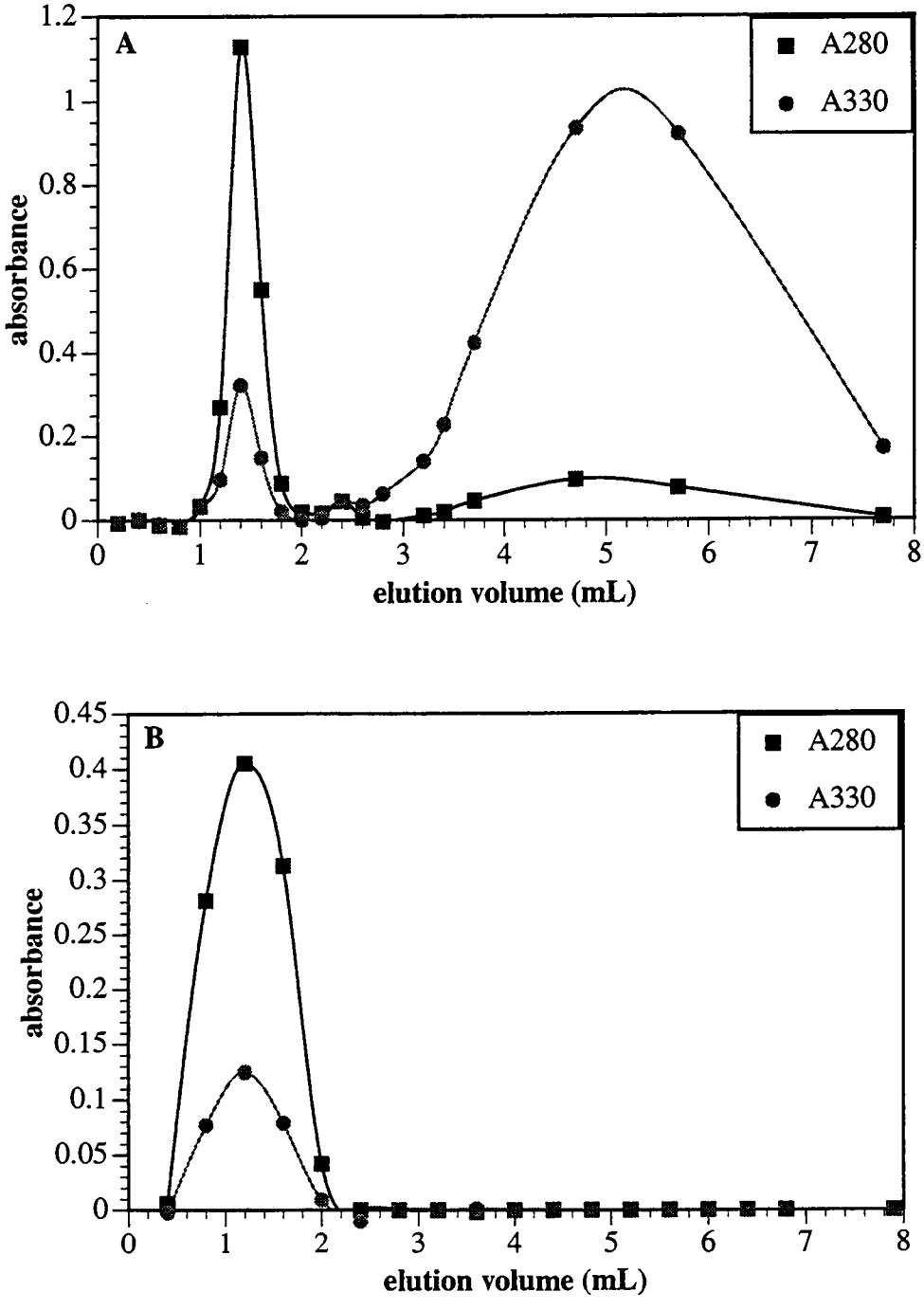

Figure 4-1: Separation of *o*-aminobenzoyl *E. coli* Trx from excess isatoic anhydride by using a Pharmacia NAP 10 column. **A** depicts the elution profile of the original reaction mixture. In **B**, the material from the major A_{280} peak in **A** was reapplied to the column.

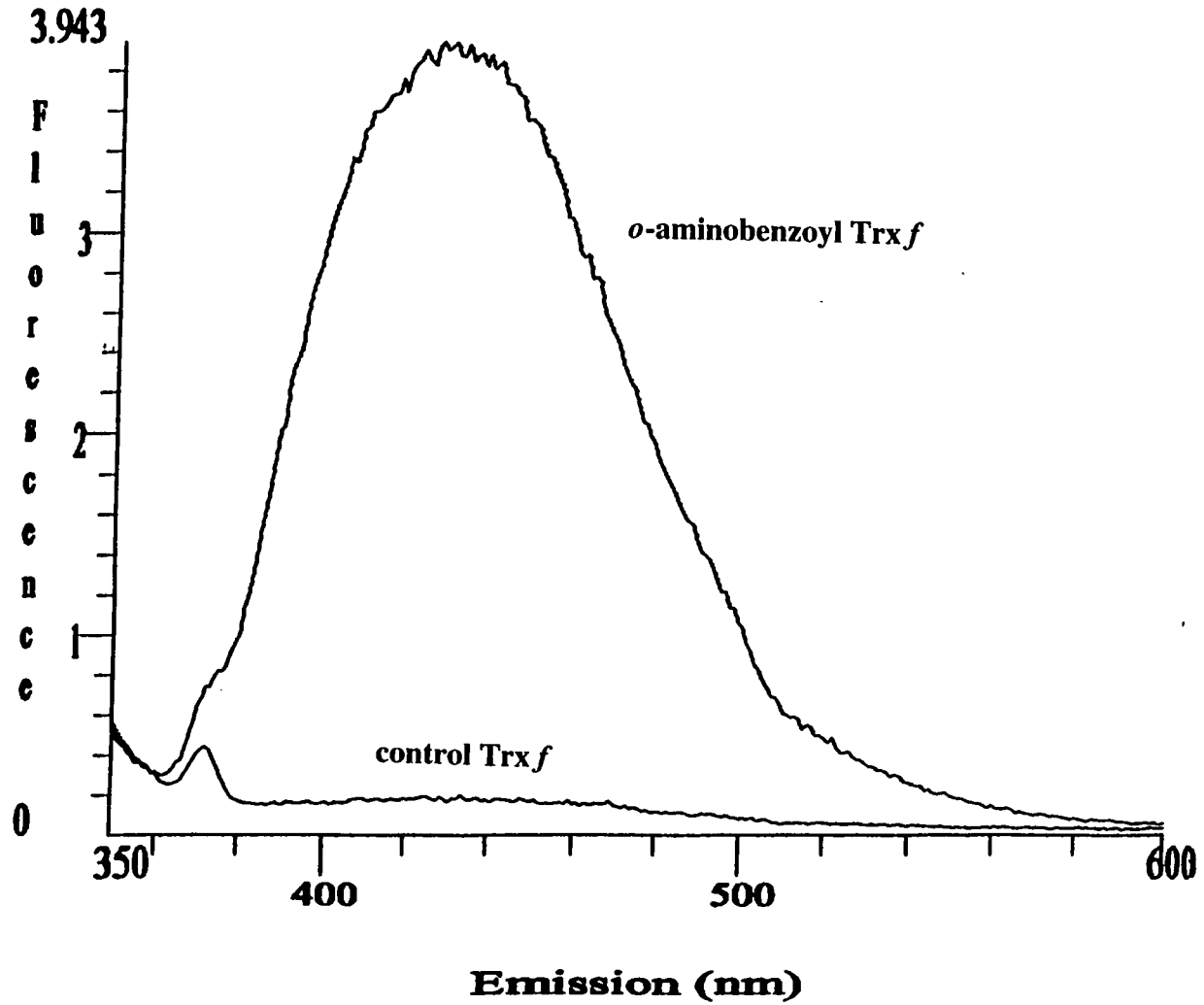

Figure 4-2: Fluorescence emission spectra of samples of *o*-aminobenzoyl Trx *f* and Trx *f* subjected to a "control" labeling reaction which were excited at 330 nm. In each case, 5 μM Trx solutions in 50 mM Bicine-KOH pH 8.0/5 mM DTT were analyzed.

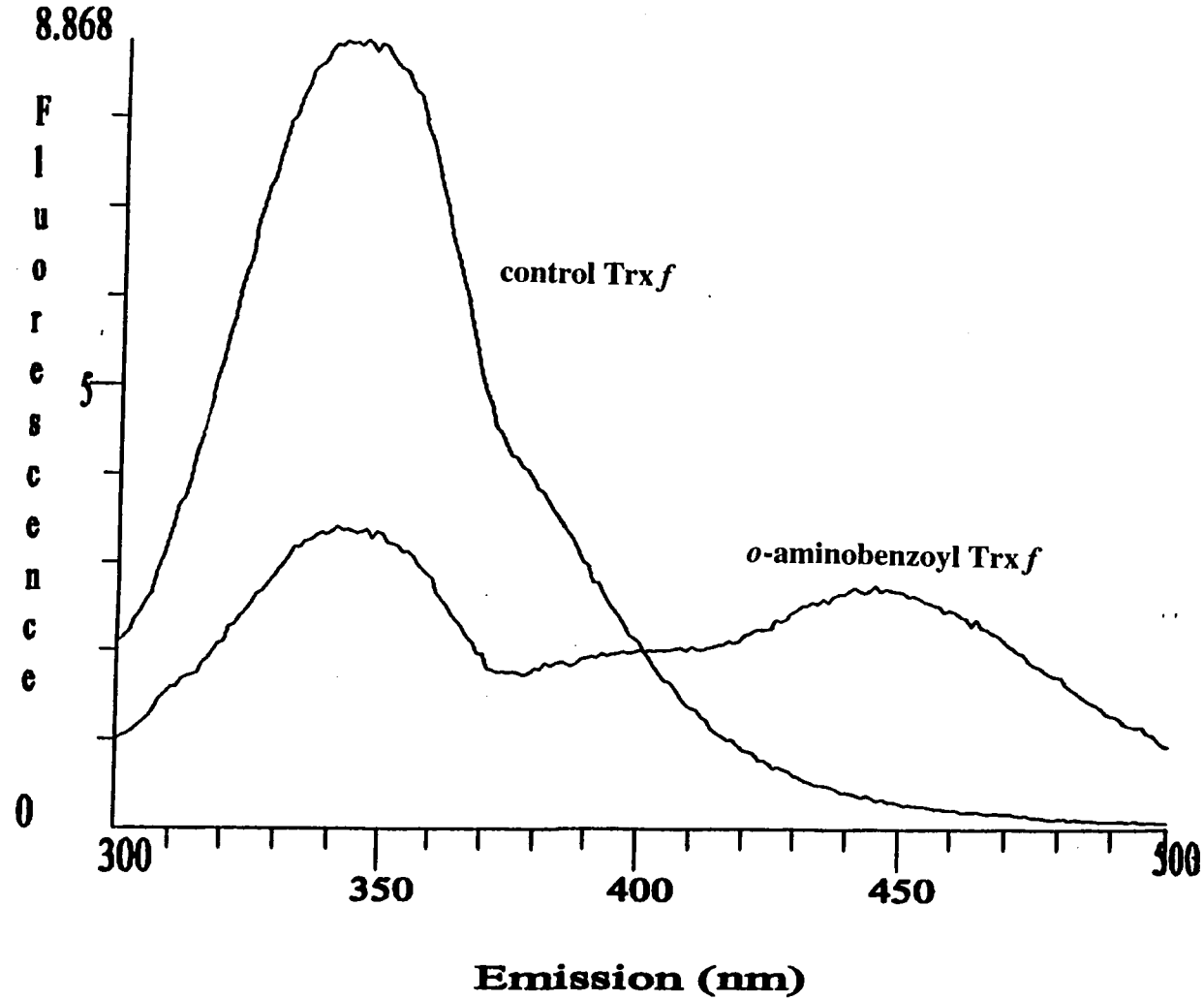

Figure 4-3: Fluorescence emission spectra of samples of *o*-aminobenzoyl Trx *f* and Trx *f* subjected to a "control" labeling reaction which were excited at 280 nm. In each case, 5 μM Trx solutions in 50 mM Bicine-KOH pH 8.0/5 mM DTT were analyzed.

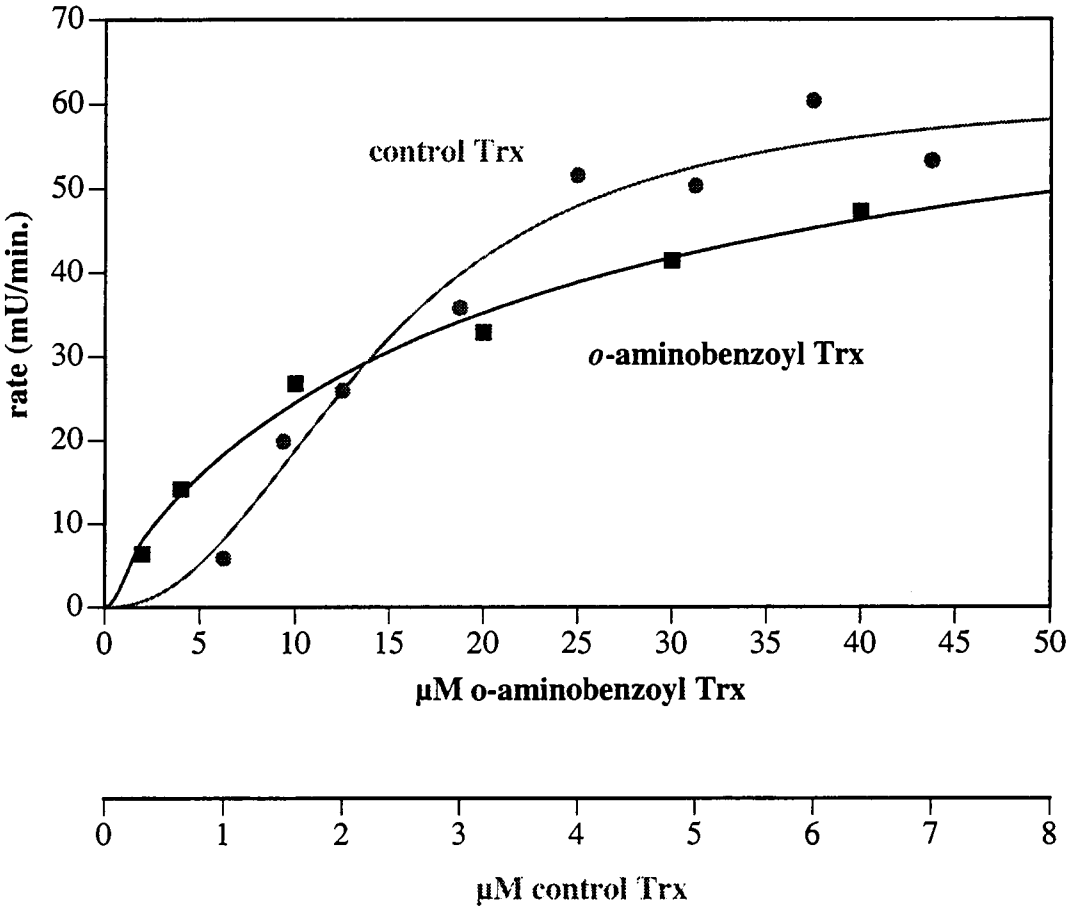

Figure 4-4: Activation of FBPase by wild-type Trx *f* subjected to the labeling reaction with isatoic anhydride. Initial rates of activation by the specified concentrations and types of thioredoxins are represented by individula data points. Data were fit to the simplified Hill equation of $v = V_{max}[S]^n/(K' + [S]^n)$, where n is a calculated value for the apparent number of binding sites.

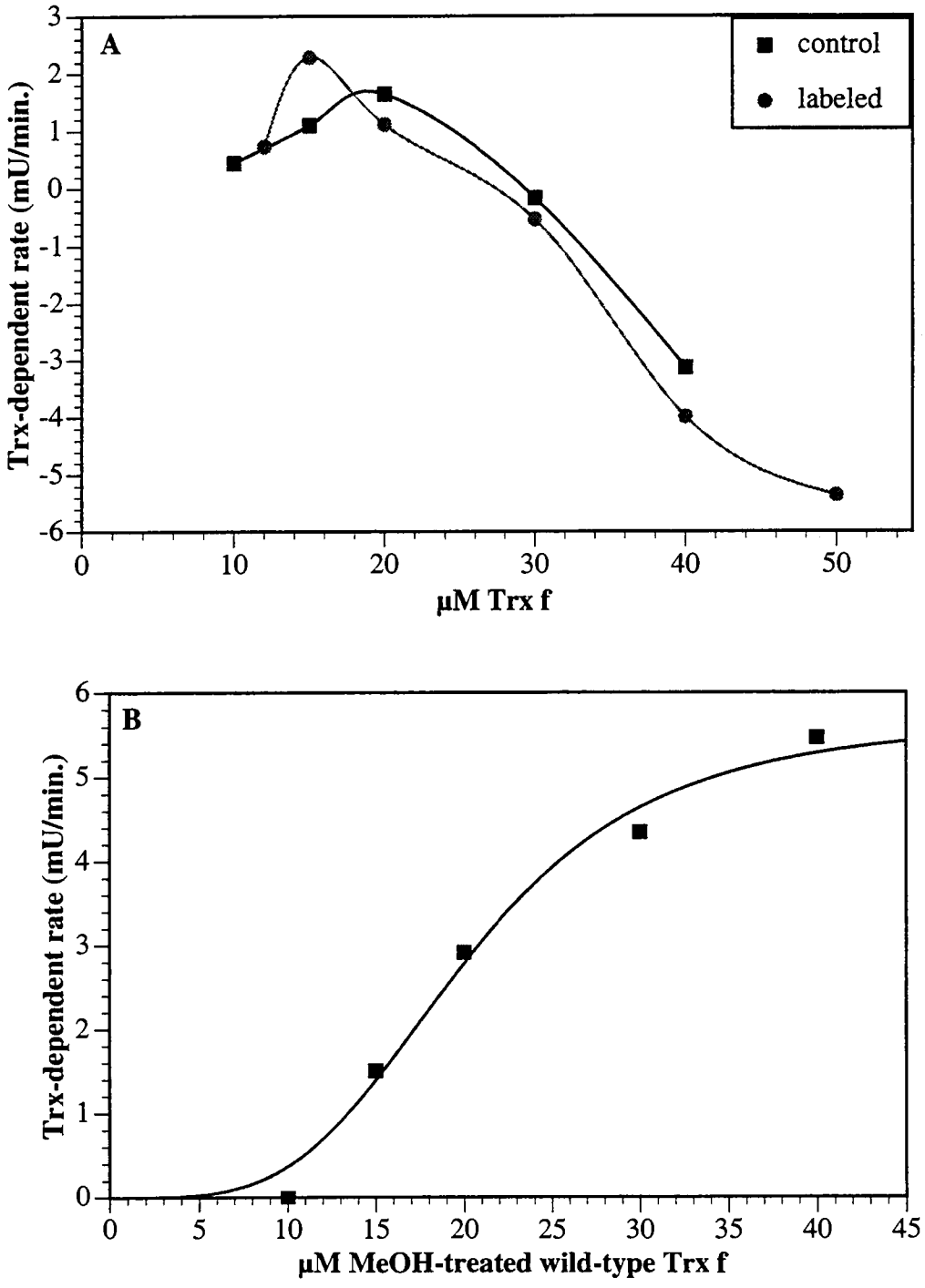

Figure 4-5: Activation of PRK by wild-type Trx *f*. In **A**, the Trx was subjected to the labeling reaction with isatoic anhydride. In **B**, the Trx was treated with 5.5% MeOH for 1 hr. at room temp. and the curve fitting was performed as in Fig. 4-4.

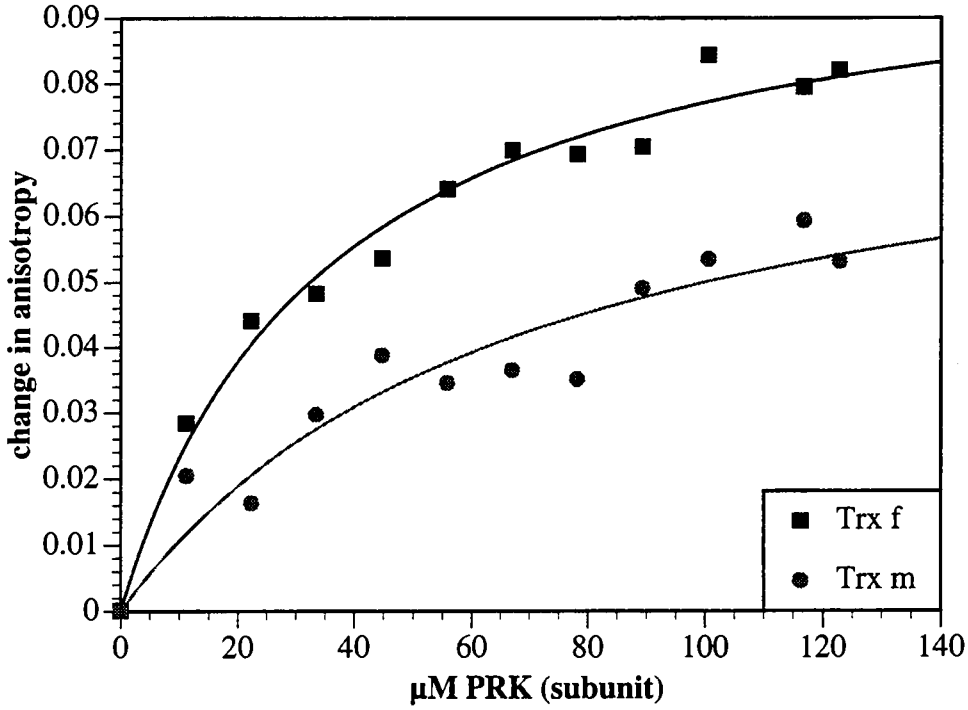

Figure 4-6: Binding of *o*-aminobenzoyl derivatives of wild-type Trx *f* and Trx *m* to PRK. For the titration, increasing amounts of oxidized PRK were added to a 3 µM solution of derivatized Trx in 50 mM Hepes-KOH pH 7.8/5 mM DTT. Following mixing with a spin flea and equilibration, anisotropy measurements were taken (1.5 sec/measurement; 5 measurements at each indicated PRK concentration), with the G factor being determined once per measurement. Each data point represents the average change in anisotropy upon addition of the indicated amount of PRK. K_d values were calculated from Michaelis-Menten curve fits using Enzfitter (Leatherbarrow, 1987).

1 M E Q A L G T Q E M E A I V G K **V T E V N K** D T F 25

26 W P I V K A A G D K P V V L D M F T Q W C G P C K 50

51 A M A P K Y E K L A E E Y L D V I F L K L D C N Q 75

76 E N K T L A K E L G I R V V P T F K I L K E N S V 100

101 V G E V T G A K Y D K **L L E A I Q A A** R S S 122

Figure 4-7: Complete amino acid sequence of recombinant spinach Trx *f*. The two peptides isolated from derivatized Trx *f* which had been digested with trypsin are indicated in *bold*.

VITA

Mary Kaye Geck was born in Bismarck, North Dakota on January 2, 1970. She attended private and public schools in Mandan, North Dakota, graduating from Mandan High School in May, 1988. She enrolled at Iowa State University in Ames, Iowa in August of 1988 from which she received a Bachelor of Science in Biochemistry in May, 1992. In August of 1992 she began her graduate studies at the University of Tennessee-Oak Ridge Graduate School of Biomedical Sciences located within the Biology Division (now known as the Life Sciences Division) of Oak Ridge National Laboratory, receiving her Doctor of Philosophy degree with a major in biomedical sciences in August, 1997. Following graduation, she will be working as a postdoctoral research fellow in the Department of Molecular and Cell Biology at the University of California-Berkeley.